

## **CHAPTER 2**

### **LITERATURE REVIEW**

This chapter deals with a critical review literatures on synthesis of different nanoparticle using chemical and green route, advantages of green synthesis over chemical synthesis. Application of different parts of plants as reducing agent/ capping agent/ stabilizing agent for synthesis of different types of nanoparticles, their mechanism and application were discussed in details. Second half of this section will cover the review literature on nanocomposite film/membrane where effect of adding green synthesized nanoparticles on the performance of polymer film/membrane for wastewater treatment will be highlighted. Lastly the chapter emphasis on the different techniques available to remove Cr(VI) from wastewater and their comparison with respect to their performances as obtained from the experimental result done by researchers also the effect various factors affecting the properties and performances of photocatalytic membrane were also reviewed.

#### **2.1 NANO-PARTICLES: PREPARATION AND APPLICATIONS**

Over the past three decades nanotechnology has evolved as an independent field with numerous applications in diverse areas. Dimension less than  $1/10^{\text{th}}$  of micro is called a nano size dimension for example  $0.1\mu\text{m}$  is equal 100nm, thus particles of materials smaller than 100 nm are commonly defined as nanoparticles. These are very small size particles with excellent catalytic reactivity, chemical steadiness, and non-linear optical performance owing to their large surface area to volume ratio (Agarwal et al., 2017). Biological, chemical and physical methods are used to synthesize nanoparticles. The physical methods are costly and high temperature and pressure conditions are needed to obtain particles in nano range. On the other hand chemical methods need

toxic chemicals which may be hazardous both for the environment as well as person handling it. Also most of the toxic chemical consumed cannot be recycled, reused or degraded to harmless forms (Agarwal et al., 2017). The capping and stabilizing agents may be needed to prevent agglomeration of nano-particles prepared through physical and chemical methods which add additional cost to the synthesis process. Synthesis of particle using plant extract or micro-organism termed as “Biosynthesis”. It is cheap and easy to carry out and has been widely used in recent years (Agarwal et al., 2017). The schematic representation of nano-particle formation using green approach is shown in Figure 2.1

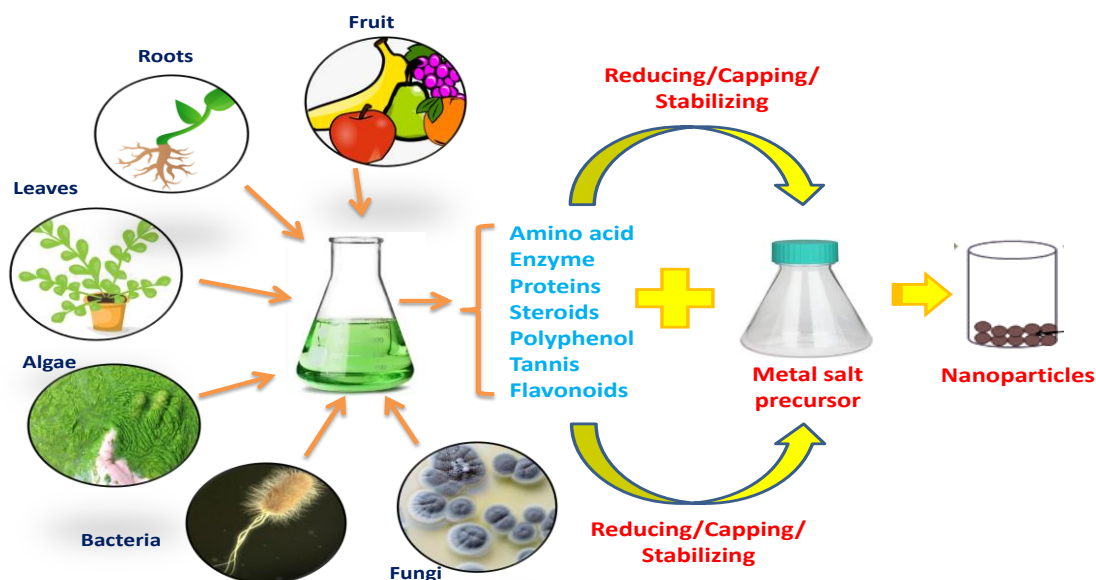


Figure 2.1: Schematic representation of the green synthesis of nano-particles

This approach for particle synthesis is advantageous in terms of cost, biocompatibility, safety and environmental friendliness. Use of different parts of plant extracts over micro-organisms (bacteria and fungi) are preferred for nano-particle synthesis because of the faster rate of biosynthesis, and possibility of large scale of production without maintaining any stringent conditions which are necessary in case of

micro-organisms (Sharma et al., 2019). Considering the advantages of plant extract over micro-organism, physical and chemical methods numerous nano-particles have been synthesized using extract from different parts of plants.

As mentioned earlier nano-particles have found applications in diverse fields ranging from agriculture, chemical industry etc. to healthcare and environmental remediation. Some typical applications also include as nano carrier for drug delivery, as catalyst for dye reduction (Srikar et al., 2016), photocatalytic systems, solar cells (Pawar et al., 2019)

During the past two decades interest in use of nano-particles as photo-catalysts for oxidizing organic air and water pollutants have increased as evidenced from some recent reviews (Kanan et al., 2019; and Reddy and Kim, 2015). Pesticides, a pernicious chemical to humankind offer a difficulty to treat them by conventional method due to their strong recalcitrant nature. However photochemical approach leads to mineralization of pesticide. Photochemical approach uses utilization of light radiation as energy source to generate reactant molecule to carry out degradation of pesticides (Reddy and Kim, 2015). Degradation of pesticide and other organic pollutant using photocatalysis has a potential alternative to traditional water treatment technique (Kanan et al., 2019). This study highlights the recent advancement in photocatalytic degradation of pollutant using TiO<sub>2</sub> based photocatalyst.

## **2.2 Nano-particles as Photo-catalysts**

The present work is focused primarily on the synthesis of nano-particles through the green route and their use as a membrane bound photo-catalyst. In view of this in the following pages a brief review of latest research publications in this area is presented.

Yallappa et al. (2015) used extract of *Jasminum sambac* to prepare Au, Ag, Au–Ag alloy NPs. Wang et al. (2014) synthesized iron–polyphenol NPs using extract of *Eucalyptus tereticornis*, *Melaleucane sophila* and *Rosemarinu sofficinalis* which was successfully used as catalyst to degrade Acid Black-194 dye.

Several organic compounds such as 4-nitrophenol (4-NP), methyl orange (MO), congo red (CR) and methylene blue (MB) were also reduced photo catalytically using Ag/TiO<sub>2</sub> nano-composite prepared by the extract of *Euphorbia heterophylla* leave. The synthesized catalyst retained its efficiency even after 5<sup>th</sup> cycles (Atarod et al., 2016). Plants of Lamiaceae family e.g. *Anisochilus carnosus* (Anbuvaran et al., 2015), *Plectranthus amboinicus* (Fu and Fu, 2015) and *Vitex negundo* (Ambika and Sundrarajan, 2015) have been extensively studied for –preparing metallic NPs of different sizes and shapes like spherical, quasi-spherical, hexagonal, and rod-shaped. Presence of compounds like phenolic acid, flavonoids, alkaloids and terpenoids, all secondary metabolites are mainly responsible for the formation of metallic nanoparticles by reduction of the ionic precursor (Aromal and Philip, 2012).

Patidar and Preeti (2017) reported the synthesised of TiO<sub>2</sub> NPs of crystallite size 12.22 nm using extract of *Moringa oleifera*, commonly known for its good antibacterial, anti-septic, and anti-inflammatory activities. The leaf extract of *Psidium guajava* was used as the reducing and capping agent to prepare copper oxide nano-particles using from copper acetate monohydrate as precursor (Singh et al., 2019). The average size of particle ranged from 2–6 nm with BET surface area of 52.6 m<sup>2</sup>/g. The Particle catalytic efficiency was evaluated in terms of % degradation of the industrial dyes, i.e., Nile blue (NB dye) and reactive yellow (RY) and achieved 93% removal of NB dye and 81% removal of RY in 120 min was achieved. An efficiency removal of 75% dye was

obtained using green synthesized TiO<sub>2</sub> NPs. The spherical shape TiO<sub>2</sub> particles of size 50-120nm were prepared using extract of *Acacianilotica* and a removal of 75% dye was obtained using green synthesized TiO<sub>2</sub> NPs (Kazi et al., 2019). Likewise Palladium NPs obtained from *Cotton boll peels* of average size ranging from 9 nm of spherical shape showed good catalyst activity against toxic azo dye (Narasaiah and Mandal 2020). Nabi et al. (2020) also mentioned the photocatalytic activity of TiO<sub>2</sub> NPs of size 80 nm (spherical shape) using Lemon peel extract. The same application was also reported by Arabi et al. (2020) where the TiO<sub>2</sub> particle was synthesized using *Alcea* and *Thyme* plant extract having size 10 nm but polyhedron and irregular shape. Degradation of methyl blue dye was mentioned in the study by Sheik Mydeen et al. (2020) using ZnO NPs prepared using plant extract of *Prosopis juliflora* of irregular shape and size 31 nm.

Nano-particle catalysts have also found wide variety of application for removal of heavy metal from wastewater. Sethy et al., 2020 synthesized low-cost indigenous TiO<sub>2</sub> powder using an aqueous solution of *Syzygium cumini* leaf extract acting as a capping agent and titanium isopropoxide (TTIP) as precursor material. The synthesized TiO<sub>2</sub> nanoparticle of crystallite size 10 nm, with a large Brunauer-Emmett-Teller (BET) surface area of 105 m<sup>2</sup>/g was used to evaluate the photocatalytic removal efficiency of particle against lead from explosive industrial wastewater. The experiments were performed in a self-designed reactor. Inductive coupled plasma spectroscopy (ICP) was used to determine the lead concentration and the obtained results witnessed 75.5% removal in chemical oxygen demand (COD) and 82.53% removal in lead (Pb<sup>2+</sup>). This application of green TiO<sub>2</sub> NPs is being explored for the first time.

Honey solution as the solvent medium/stabilizing medium was also used to synthesize calcium alginate (Geetha et al., 2016). The effective removal of 93% Cr (VI)

ions at pH 4 in 180 min was reported. List of various nano-particles synthesized via green route, their size, shape and typical application are shown in Table 2.1.

**Table 2.1: List of green route synthesized nanoparticles: Shape, size and application**

Leave Extract	NPs	Results	Reference
<i>Parthenium hysterophorus extract</i>	TiO <sub>2</sub>	Method: Microwave irradiation Average size: 20–50 nm Shape: spherical shape % degradation of dye was > 85%	Thandapani et al., 2018
<i>Azadirachta indica aqueous leaf extract</i>	Ag	Average size: 34 nm Efficient antimicrobial activities against E. coli and S. aureus.	Ahmed et al., 2017
<i>Polygala tenuifolia</i>	CdO	Shape: Trigonal Average size: 34 nm	Ghotekar et al., 2019
<i>Moringa oleifera</i>	ZnO	Spherical shape particle Average size: 6-20 nm	Agarwal et al., 2016
<i>Jatropha curcas</i>	TiO <sub>2</sub>	Average crystalline size: 13 nm Average size: 10 to 20 nm Spherical shape particle Removal of COD and Cr is 82.26% & 76.48% respectively in tannery wastewater.	Goutam et al., 2018
<i>Sesbania grandis</i>	TiO <sub>2</sub>	Average crystalline size: 42.58	Srinivasan et

<i>flora</i>		nm Shape: Triangular, square and spherical	al., 2019
<i>Fraxinus rhynchophylla</i>	ZnO <sub>2</sub>	Average diameter 100-200 nm	Wang et al., 2020
<i>Vitex agnus-castus</i>	SnO <sub>2</sub>	Average size: 4 to 13 nm Shape: spherical shape	Ebrahimian et al., 2020
<i>Cassia fistula</i> and <i>Melia azadarach</i>	ZnO	Shape: Spherical Average size: 3-68 nm	Naseer et al., 2020
<i>Citrus Limon</i>	Cu	Shape: Spherical Average size: 30 nm	Amer and Awwad 2021

### 2.3 PHOTOCATALYTIC REMOVAL OF POLLUTANT USING GREEN SYNTHESIZED NANOPARTICLES

The generalised mechanism for photo-catalytic removal of pollutant involves photo-excitation of nano-particles (Figure 2.2) to generate electron hole pair on the metal/metallic oxide surface as shown by equation 2.1



The excited electrons in the presence of O<sub>2</sub> can proceed in a single stage reduction, form a superoxide radical anion O<sub>2</sub><sup>-</sup> whereas the holes (h<sup>+</sup>) react with H<sub>2</sub>O proceed in a single stage oxidation and form hydroxyl radicals OH<sup>o</sup>. The generated radicals are highly reactive and can mineralize the substrates to CO<sub>2</sub> and H<sub>2</sub>O (Mull et

al., 2017). The generalized equations of oxidation and reduction is shown in equations (2.2) to (2.5)

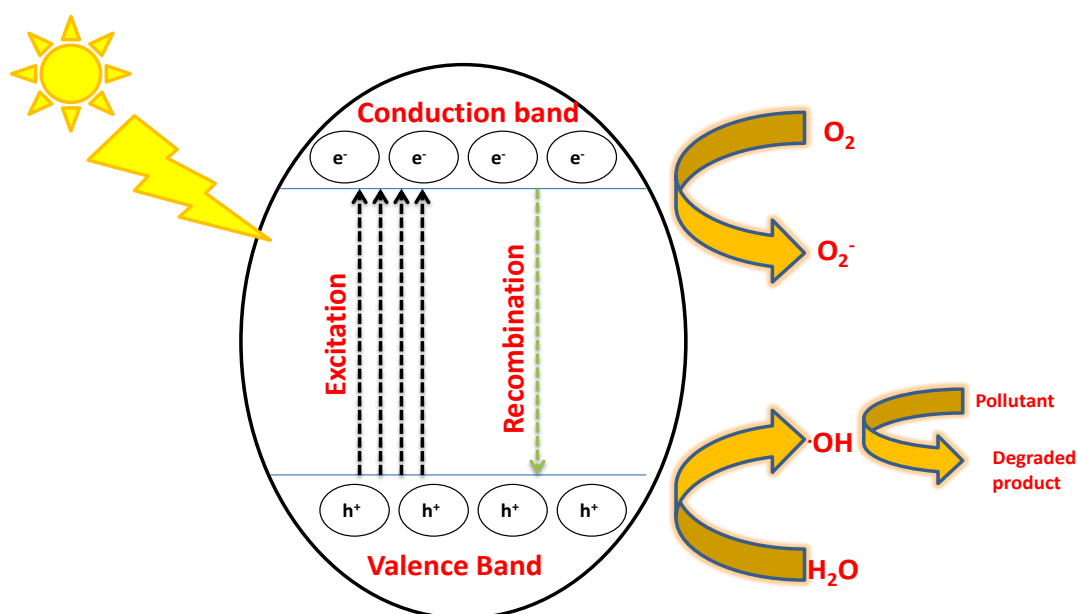


**Figure 2.2: Mechanism for photo-catalytic degradation of pollutants**

Tamuly et al. 2013 reported formation of gold nanoparticles from *Gymnocladus assamicus*. The particle exhibited excellent catalytic activity in reduction to 4-aminophenol from 4-nitrophenol. In other literature (Das and Velusamy 2014) outstanding catalytic performance was shown by gold nanoparticles extracted from *Sesbania grandiflora* plant against reduction of methylene blue dye. Similarly other nanoparticle like Pd nanoparticles were also found useful and showed excellent photocatalytic activity for phenol red dye degradation at pH 6 when experiment were performed on various pH ranging from 2 to 10. The surface plasmon resonance (SPR)



spectroscopy analysis reveals disappearance of band at 433 nm at pH 6 (Kalaiselvi et al. 2015). Likewise TiO<sub>2</sub> particle synthesized from *Syzygium cumini* also exhibit excellent photocatalytic removal of lead found in industrial wastewater (Sethy et al., 2020)

Nano-particle catalysts have also found application for removal of heavy metal from wastewater. Saravy et al. (2014) reported photo-catalytic degradation of cyanide in presence of UV light from wastewater using TiO<sub>2</sub> NPs of average size ranging from 18 to 22 nm. In other report extract of *Eucalyptus* leaf was used to prepare iron based nano-particles and used to remove mixed contaminant of Cr(VI) and Cu(II) from wastewater using the combined technique of adsorption and reduction (Weng et al., 2016). Effects of different parameters like pH, reaction temperature were discussed in detail on the removal efficiency. Mixed magnetite–hematite of size 4- 52 nm was synthesized by Ahmed et al. (2013) by the co-precipitation technique. The synthesized particles were used for removal of lead(II), cadmium(II) and chromium(III) by adsorption method. At optimum value of 7 pH, the evaluated adsorption capacity for Pb(II), Cd(II) and Cr(III) were 617.3, 277 and 223.7 mg/g, respectively which was comparatively very much high. Fazlzadeh et al. (2017) studied the effect of extracts of three different plants *Rosa damascene*, *Thymus*, and *Urtica* to synthesize zero valent iron nanoparticles and used for Cr(VI) from aqueous solution. It was concluded that 94% removal was achieved using extract of *Rosa damascene* for particle synthesis in 30 min using adsorption method.

Goutam et al. (2018) reported photo-catalytic degradation of pollutant generated from tanneries using green synthesized spherical shaped, anatase phase TiO<sub>2</sub> NPs from extract of *Jatropha curcas*. The study concluded 82.26% COD removal and 76.48% Cr(VI) removal from the tannery waste water in a self-designed fabricated Parabolic

Trough Reactor after the secondary biological treatment process was obtained. Using the same extract Magudieshwaran et al., 2019 synthesized CeO<sub>2</sub> (cerium oxide) NPs of size 18–25 nm for photo-catalytic degradation of aldehyde, an indoor gaseous pollutant. The photo-catalytic activity 99.6% of particle was obtained for acetaldehyde mineralization into CO<sub>2</sub>. The nano-composite of ZnO/NiFe<sub>2</sub>O<sub>4</sub> nano-particles was obtained using solid state synthesis and was used to eliminate contaminants from both domestic and industrial waste waters. The ZnO particles were produced using *Mangifera indica* leaf extract and anhydrous Zinc acetate as the precursor (Adeleke et al., 2018). Another composite of gold/silver/silver chloride (Au/Ag/AgCl) was prepared using *Momordica charantia* (medicinal leaves) extract (Devi and Ahmaruzzaman, 2017) to degrade clofibric acid and ibuprofen. Presence of phytochemical in leaves results in the formation of nanoparticles. A total of 98% of clofibric acid (CA) and 97% of ibuprofen (IBP) were degraded under solar radiation.

The low cost pesticides are commonly used for residential, agricultural and commercial purposes were degraded photo-catalytically in presence of sun irradiation using metal hexacyanoferrate (MHCF) nanoparticles. Particles were obtained using bio-surfactant *Sapindus mukorossi*, a commonly found plant of India. Under optimized conditions (at 50 mg L<sup>-1</sup> of pesticide neutral pH and 15 mg of MHCF photocatalyst, neutral pH), the maximum degradation of 98% pesticide was obtained (Rani and Shanker 2018). Aloe vera plant gel was also used to synthesize photo-catalytic TiO<sub>2</sub> particle (Hariharan et al., 2018) to study the degradation of picric acid (trinitrophenol). The synthesized particles having the size range of 6-13 nm of anatase phase showed higher photo-catalytic degradation of picric acid than the pristine TiO<sub>2</sub> NPs in 120 min.

Fruits extract have also been used to synthesize nano-particles by several researchers. Atchudan et al. (2018) prepared composite of TiO<sub>2</sub> NPs (TiO<sub>2</sub> nanoparticles/nitrogen-doped carbon) by hydrothermal process using peach fruit. The degradation efficiency for MB dye was found to be greater than 90% within 40 min under UV radiation. Also its zero toxicity towards the *Candida albicans* indicated its other application as life cell imaging. *Carissa edulis*, (a medicinal plant) fruit extract was utilized to synthesize ZnO NPs using microwave assisted technique Fowsiya et al., 2016. Scanning electron microscopy study depicted flower shaped morphology and particle size ranging between 50-55 nm. The photo-catalytic degradation- for Congo Red was found to be 97% after 140 min. Singh et al. (2018) reported biogenic synthesis of SnO<sub>2</sub> NPs spherical shape with average size 8.4 nm using *Piper betle* leaves extract . In presence of direct sunlight the observed photo-catalytic degradation efficiency against reactive yellow 186 dye was 92.17%. No significant change in efficiency was observed after 5th cycle of use indicating good stability and reusability of particles. Green synthesized pH responsive Al<sub>2</sub>O<sub>3</sub> NPs were synthesized using *Prunus x yedoensis* leaf extract through the biological reduction method. The obtained particles were of size 50-100 nm and were of spherical and hexagonal shape. The particles showed a high catalytic efficiency of 94% for nitrate removal at neutral pH under solar irradiation (Manikandan et al., 2019). Table 2.2 summarizes the particles synthesized by green route and used for photo-catalytic application.

**Table 2.2: Summary of NPs synthesized by green route for photocatalytic application**

Particle	Extract	Results	Reference
Gold nano-particles	<i>Lagerstroemia speciosa</i> leaf extract (LSE)	<ul style="list-style-type: none"> <li>• Acidic pH of 2 most favorable for AuNPs bio-synthesis at 100 <math>\mu</math>L of 4% LSE and 50 ppm gold solution .</li> <li>• Diameter in the range of 107–193 nm.</li> <li>• Reduction efficiency of <math>\geq 90\%</math> for MB, MO, BPB (bromophenol blue), BCG (bromocresol green), and 4-NP (nitrophenol)</li> </ul>	Choudhary et al., 2017
Zinc oxide	<i>Abelmoschus esculentus</i> Mucilage	<ul style="list-style-type: none"> <li>• Formation of hexagonal wurtzite ZnO.</li> <li>• Average size: 29–70 nm</li> <li>• 125 mg of the catalyst removes 100% MB after 60 min whereas 100 mg catalyst is required for complete removal of rhodamine B within 50 min</li> </ul>	Prasad et al., 2019
Zinc oxide	Lemon juice	<ul style="list-style-type: none"> <li>• Hexagonal wurtzite with some honed faces</li> <li>• Obtained band gap energy was 3.15 eV</li> <li>• After 70 min 91.17% of MB dye, 98% rhodamine B and 90% Congo red degradation were obtained</li> </ul>	Prasad et al., 2018

Silver particles	<i>C. japonicum</i> (stabilizer agent)	<ul style="list-style-type: none"> <li>• Spherical shape without any aggregation.</li> <li>• Size: 2-8 nm</li> <li>• Photocatalytic degradation of 98% was obtained against bromo phenyl blue in 12 min.</li> <li>• In addition AgNPs adapted electrode exhibit electro-catalytic properties to reduce hydroquinone</li> </ul>	Khan et al., 2016
Iron hexacyano-ferrate	<i>Sapindus mukorossi</i> .	<ul style="list-style-type: none"> <li>• Size range: 10–60 nm</li> <li>• Shape: hexagonal, rod and spherical shape</li> <li>• At optimised condition PAHs (anthracene, phenanthrene, chrysene, fluorene, and benzo (a) pyrene): 50 mg L<sup>-1</sup>, catalyst dose: 25 mg, neutral pH and solar – irradiation: 80 to 90% degradation was observed for Anthracene and phenanthrene, whereas ~70-80% was observed for fluorene, chrysene and benzo (a) pyrene were</li> </ul>	Shanker et al., 2017
SnO <sub>2</sub>	<i>Vitex agnus-castus</i> fruit	<ul style="list-style-type: none"> <li>• Size range : 4 to 13 nm</li> <li>• Shape: spherical shaped particle</li> <li>• Degradation of rhodamine B (RhB) : 91.7% in 190 min</li> <li>• Removal of heavy-metal ions Co<sup>+2</sup> &gt; 94% after 60 min</li> </ul>	Ebrahimian et al., 2020

Zinc oxide	<i>Thymus vulgaris</i> extract	<ul style="list-style-type: none"> <li>• Size of the nano-particles &lt; 40 nm</li> <li>• Shape: spherical and partly irregular</li> <li>• 95% Cr(VI) reduction, using methanol as hole scavenger at optimum condition : catalyst dosage 15 mg/L, pH 7.</li> </ul>	Khosravi et al., 2019
ZnO	Loquat seed extract	<ul style="list-style-type: none"> <li>• Size of the nano-particles &lt; 50 nm</li> <li>• Shape: hexagonal wurtzite structure</li> <li>• Highest MB dye degradation at 12 mg/ml particle concentration</li> </ul>	Shabaani et al., 2020
Silverferrite particles	<i>Amaranthus blitum</i> leaf aqueous extract	<ul style="list-style-type: none"> <li>• Average size of the nano-particles 63 nm</li> <li>• Shape: Spherical</li> <li>• 95% degradation of 120 ppm caffeine in wastewater</li> </ul>	Muthukumar et al., 2020

## 2.4 NANOCOMPOSITE FILM/MEMBRANE

Photo-catalysis, one of the attractive advanced oxidation processes to remove pollutants from environment is one of the emerging technologies. Use of nano-material as a photo-catalyst is in great demand and large number of researches have been carried out in this field. No doubt use of nano-particle in suspension form shows excellent photocatalytic efficiency due to large surface area, porosity and large number of active sites between nanoparticle surface and pollutant species which accelerates the mass transfer process. In spite of such advantages, the major drawback associated with it is

the particle recuperation from the suspension before reusing the treated water. This separation process is not only time consuming but also requires expensive downstream filtering, post-treatment thereby restricting the application of particle on wider scale (Martins et al., 2016). An alternative to resolve this issue is immobilization of particles on the solid surface. Several substrates have been tested as support for the catalyst. These include sand, paper, zeolites, ceramic membrane, pyrex, cement beads, alumina clays and steel mesh etc. However use of polymeric materials are not only gaining interest as substrate but also being used widely for membrane separation application (Zinadini et al., 2014) because of ease of processing, easy availability and cost effectiveness of the material. Along with photo-catalysis, membrane separation is also an emergent technology that has great potential for wastewater treatment.

The major drawback faced using membranes made out of pure polymers is their high fouling tendency thereby reduction in the permeation flux as well as requirement of frequent cleaning and/or replacement of membrane leading to high operational and maintenance costs (Zinadini et al., 2014). To overcome this problem concept of fabrication of “nano-composite film/membrane” came into picture. The nano-composite film may be defined as incorporation/immobilization of nano-particle within the polymer matrix/substrate. Use of nano-composite membranes takes care of the problems faced using suspended form of particles as well as those using the pristine polymer.

Gong et al. (2009) fabricated multi-wall carbon nano-tube and iron oxide nanoparticles nano-composite for the removal of cationic dyes. Daraei et al. (2013) prepared thin film composite membrane composed of nanoclay/chitosan on PVDF and used for microfiltration application for the removal of organic dye from an aqueous solution. It was concluded that Acid Orange 7 dye was very well removed by chitosan

coated membrane at acidic pH. Zinadini et al. (2014) fabricated a nano-filtration membrane using carboxy methyl chitosan coated  $\text{Fe}_3\text{O}_4$  nano-particles and used it for the removal of Direct Red 16 dye. The synthesized nano-composite membrane showed an increase in flux from 9.2 to 36  $\text{kg/m}^2\text{h}$  with increase in dye removal percentage from 88 to 98.5%.

A membrane composed of cellulose nanocrystal/chitosan was synthesized by Karim et al. (2014) for the removal of positively charged dyes through ultra-filtration. The membrane of pore size ranging from 13-17 nm effectively removed 99% of the dye. The hybrid nano-filtration membrane of halloysite nano-tubes/polyethersulphone prepared via distillation–precipitation polymerization method showed higher rejections above 90% for Reactive Black 5 and 80-90% for Reactive Red 49 (Wang et al., 2015).

Nano-composite membrane consisting of graphene oxide quantum dots incorporated in a tannic acid matrix was prepared by interfacial polymerization and was used for nano-filtration. This membrane showed improved flux upto 1.5 times higher than the pristine membrane (Zhang et al., 2017). In addition to it, membrane also exhibited good antifouling property with 99.8% rejection of Congo Red and 97.6 % for Methylene Blue. Yang et al. (2017) used a combination of self-assembly and interfacial reaction for the synthesis of nano-filtration membrane composed of zeolite imidazolate/polyethyleneimine. The fabricated membrane showed increase in permeance from  $12.6 \text{ L m}^{-2} \text{ h}^{-1} \text{ bar}^{-1}$  to  $42.0 \text{ L m}^{-2} \text{ h}^{-1} \text{ bar}^{-1}$  and an increment in rejection from 72.3 to 94.4%. Peyraj et al. (2014) synthesized thin film nano-composite membrane for separation of dye. It was concluded that  $\text{TiO}_2$  loading on the membrane plays a crucial role in affecting the performance of the membrane as the highest rejection rate of 94.7% was obtained for Bromothymol Blue (BTB). Rahimpour et al. (2008) reported effect of



UV irradiation on the PES membrane incorporated with TiO<sub>2</sub>/PES NPs and concluded that the presence of NPs enhances the flux and fouling resistance in presence of UV irradiation due to the superhydrophilicity of TiO<sub>2</sub>. Damodar et al. (2009) reported that a superior membrane with enhanced permeability, fouling resistance and high antibacterial capability in PVDF membrane was obtained when TiO<sub>2</sub> was used as filler.

Effluents containing heavy metal were also treated using membrane separation. Removal of arsenate using nano-composite ultra-filtration membrane was reported by Gohari et al. (2015). Nano-composite membrane of polyethersulfone (PES) and titanate nanotubes (TNTs) was fabricated to overcome the limitation of adsorption process. It was observed as the weight ratio of TNTs: PES when increased from 0 to 1.5 the water permeability increased from 39.4 to 1250 L m<sup>-2</sup> h<sup>-1</sup> bar<sup>-1</sup> and a high quality permeate was generated to meet the World Health Organization (WHO) standard of the permissible limit of As (<10 µg L<sup>-1</sup>).

Presence of excess Cu(II) in body may lead to abdominal diseases for e.g. nausea, vomiting and diarrhea. Study on Cu(II) removal by ultra-filtration membrane was reported by Chan et al. (2015). They fabricated PEG-coated Co-Fe<sub>2</sub>O<sub>3</sub> in PES nano-membrane and obtained 96% of Cu(II) removal using nano-modified membranes. Daraei et al. (2012) reported Cu(II) removal efficiency of 85% without considerable decline in rejection even after 5 runs using a membrane composed of polyethersulfone (PES) and polyaniline/iron(II,III) oxide (PANI/Fe<sub>3</sub>O<sub>4</sub>) nanoparticles prepared by the phase inversion method. Ghaemi et al., (2016) prepared γ-alumina nanoparticles embedded PES polymer membrane. The membrane resulted in improved hydrophilicity, porosity and water flux and negligible change in rejection (<4%) was observed even after four runs of filtration.

A bio-based membrane of cellulose microfibril/cellulose nanocrystals in a gelatine matrix was synthesized by Karim et al. (2016) to remove heavy metal ions from mirror industry effluent. Microfiltration membrane of pore size 5.0–6.1  $\mu\text{m}$  showed a significantly high water flux value 900–4000  $\text{L h}^{-1} \text{m}^{-2}$  at 1.5 bar. The heavy metal removal is attributed to the ionic interaction due to the presence of negatively charged nano-cellulose and the positively charged metal ions. An effluent consisting of multiple ions was successfully treated using membrane filtration application. A novel mixed matrix membrane was fabricated by the phase inversion technique using polysulfone (PSf)/ $\text{Fe}_3\text{O}_4$ . Increased lead (II) and nickel (II) rejection was observed with increase in  $\text{Fe}_3\text{O}_4$  loading from 7 to 9 wt%. However further increase in loading produced negative impact on the membrane due to the macro void formation in membrane structure (Moradihamedani et al., 2016). A summary of the available information on the use of nanocomposite membrane for pollutant removal is shown in Table 2.3

**Table 2.3: Nano-composite membranes for pollutants removal**

Nanocomposite membrane	Synthesized/ Commercial	Results	Reference
PSf/ $\text{TiO}_2$ -GO	Synthesized	• Compare to pure PSf degradation of MB is about 60–80% faster	Gao et al., 2014
PVDF@ $\text{CuFe}_2\text{O}_4$ catalytic membrane	Synthesized	• Separation efficiency is 99.77% to MB, 81.02% to RhB, 36.35% to HA, and 82.94% to BSA	Wang et al., 2019
PVDF/ graphene oxide and $\text{TiO}_2$	Synthesized	• Photo-degradation efficiency improved by 50–70%. water flux is more than 2 times	Xu et al., 2016

		that of the pristine PVDF membrane,	
PAN/ PVP/ TiO <sub>2</sub> nanoparticles	Synthesized	<ul style="list-style-type: none"> <li>• Separation percentage for COD, BOD, detergent and TSS is 92,91,90 and 97% respectively</li> </ul>	Ejraei et al., 2019
PVA/TiO <sub>2</sub> /graphene-MWCNT	Synthesized	<ul style="list-style-type: none"> <li>• Photo-catalytic decomposition was more than 70%</li> <li>• Activity was maintained more than 90% even after three cycle</li> </ul>	Jung et al., 2014
Graphene Oxide/ ethylenediamine / poly-ethylenimine	Synthesized	<ul style="list-style-type: none"> <li>• High water permeability : 5.01 L m<sup>-2</sup> h<sup>-1</sup> bar<sup>-1</sup></li> <li>• Rejection % for lead, Zinc, cadmium and nickel &gt;95%</li> </ul>	Zhang et al., 2015
Polypyrrole PPy@Al <sub>2</sub> O <sub>3</sub>	Synthesized	<ul style="list-style-type: none"> <li>• Copper removal up to 81%.</li> </ul>	Ghaem et al., 2016
Sulfonated Pentablock Copolymer	Synthesized (nano-filtration)	<ul style="list-style-type: none"> <li>• Membrane effective pore diameter of 0.50 nm.</li> <li>• Molecular weight cut off: 255 Da.</li> <li>• % Rejection Pb<sup>2+</sup>, Cd<sup>2+</sup>, Zn<sup>2+</sup>, and Ni<sup>2+</sup> with a rejection of &gt;98.0%</li> </ul>	Thong et al., 2014
Polyetherimide/porous activated bentonite clay	Synthesized (Ultrafiltration)	<ul style="list-style-type: none"> <li>• Increase in porosity from 39 to 61% as clay content increase from 0 to 4%.</li> <li>• Rejection % : 69.3%, 76.2% and 82.5% for 250 ppm of Cd(II), Ni(II) and Cu(II) ion</li> </ul>	Hebbar et al., 2014

		solutions	
Activated montmorillonite/polyethersulfone	Synthesized	<ul style="list-style-type: none"> <li>• Good selectivity for elimination of <math>Zn^{2+}</math> and <math>Ni^{2+}</math> of approximately 75 and 60% compared to <math>Cu^{2+}</math> and <math>Cd^{2+}</math></li> </ul>	Mahmoudian et al., 2018
PAN-PVA membranes	Synthesized	<ul style="list-style-type: none"> <li>• Adsorption capability against Cr (VI) was 66.5 mg/(g membrane) and 33.6 mg/(g membrane) against Cd(III)ion.</li> <li>• Regeneration efficiency was above 90% after 3 cycles</li> </ul>	Liu et al., 2020
PVDF-GO	Synthesized	<ul style="list-style-type: none"> <li>• MB dye removal efficiency of 83.5 % was achieved</li> </ul>	Alyarnezhad et al., 2020
PANI-GO modified PVDF	Synthesized	<ul style="list-style-type: none"> <li>• Flux recover ratio was about 94%</li> <li>• Removal efficiency for Allura red is 98% and Methyl orange is 95%</li> </ul>	Nawaz et al., 2021
PVDF/lead doped zinc oxide	Synthesized	<ul style="list-style-type: none"> <li>• High color removal rate (98%) for reactive Black 5 textile dye</li> </ul>	Chamam et al., 2020

## 2.5 REMOVAL OF HEXAVALENT CHROMIUM (Cr(VI))

The hexavalent chromium (Cr(VI)) is in the priority list of toxic inorganic pollutants. It is proven to be mutagenic, carcinogenic and more toxic than trivalent chromium. As a result a large number of researchers across the globe have explored the efficacy of various remediation techniques for the removal of Cr (VI) as shown in Figure 2.3.

Fellenz et al. (2017) reported removal of Cr(VI) by adsorption- reduction technique. Amino functionalized sorbent was used for its removal and it was concluded that 86.4 % Cr(VI) was eliminated and 61% of Cr(VI) was reduced at acidic pH. Souza et al. (2016) in their study used macro-alga *Sargassum cymosum* as electron donor for the reduction of Cr(VI) to Cr(III). Due to the presence of negatively charged functional groups on the surface marine algae act as binding sites for metal cations. It was observed that for every 1 g of biomass 3 mmol of Cr(VI) was reduced. The mechanism for reduction was biomass oxidation during reduction of Cr(VI) generates new binding sites responsible for trivalent chromium removal.

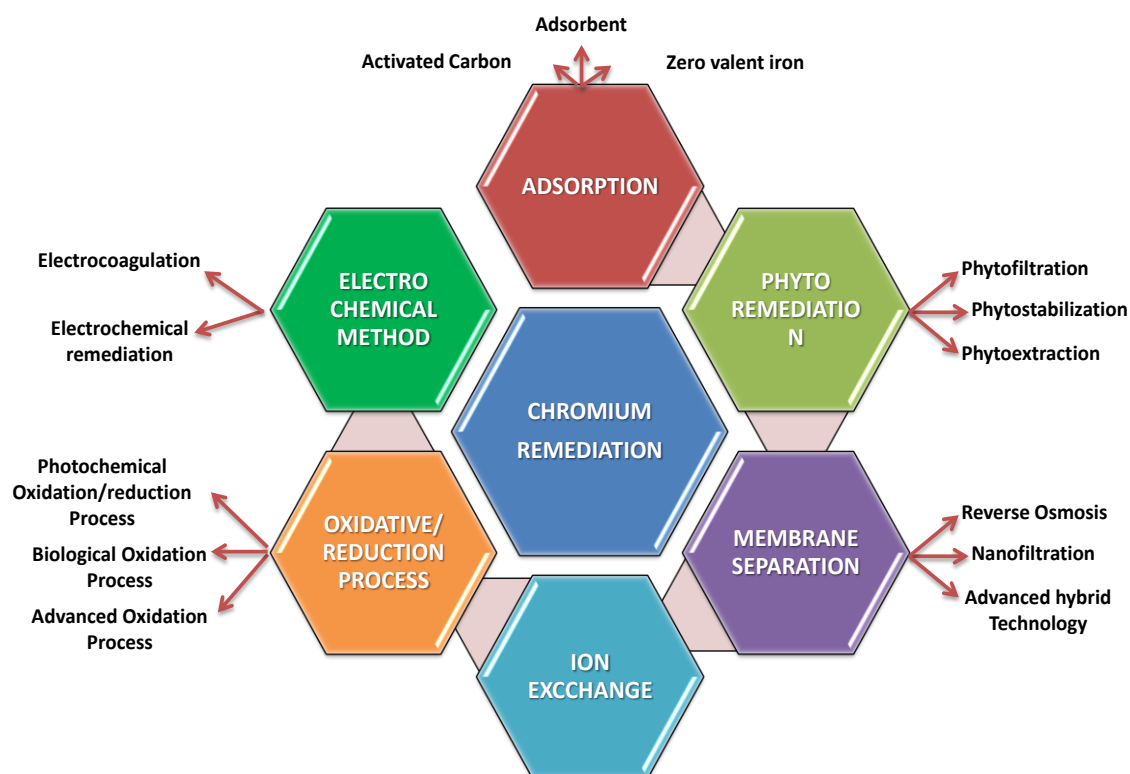


**Figure 2.3: Different techniques for remediation of chromium contaminated water**

Adsorption is considered as the most effective and economical technique for remediation of Cr (VI). Activated carbon (AC) is the most commonly used adsorbent

due to its high porosity, mechanical strength and high internal surface area however it is useful only for low concentrations of effluent stream. Acharya et al., (2009) prepared AC from Tamarind wood activated with zinc chloride and obtained 99% removal efficiency of Cr(VI) from wastewater. Fox nutshell activated by zinc chloride was also used to prepare AC and it showed a maximum removal efficiency of Cr(VI) 99.08% at acidic pH (Kumar et al., 2017). At the optimum condition (acidic pH 2, biomass dosage 2.5 g/100 ml and time of 150 min) the removal rate for Cr(VI) was observed to be 7.8 mg/g using AC prepared from mango kernel and activated with H<sub>3</sub>PO<sub>4</sub> (Rai et al., 2016). Silica-based adsorbents were also used on large scale because of the availability of both reduction and sorption capabilities in a single solid. Kumar et al. (2007) reported 85% removal of Cr(VI) and 70% removal of total chromium using aniline formaldehyde condensate attached on the silica and also 56% chromium recovery was obtained from the adsorbent in the presence of NaOH.

Considering the poor removal efficiency and high volume of spent carbon generation, electrochemical oxidation was considered as a highly efficient technique for Cr(VI) removal. Xue et al. (2017) uses graphitized MWCNTs for Cr (VI) from wastewater employing alkaline electrochemical oxidation technique. Tezcan Un et al., (2017) studied the recovery of an electroplating wastewater by electro-coagulation. At the optimum conditions (NaCl electrolyte: 0.05 M, 20 mA cm<sup>-2</sup>, and acidic pH 2.4), the 19 mM Cr(VI) concentration was completely removed consuming energy of 2.68 kWh m<sup>-3</sup>. The generated sludge was further used as raw material to manufacture inorganic pigments. Kononova et al. (2015) used cation and anion exchangers with long chained cross-linking agents and reported 100% chromium and manganese recovery in counter-current columns at initial concentrations of 0.02 and 0.09 M, respectively.

Membrane separation process is yet another emerging technology that is widely being explored and used for heavy metal removal. Out of different membrane separation alternatives- ultrafiltration, reverse osmosis, electrodialysis, and nanofiltration, reverse osmosis (RO) is considered as one of the most efficient process to remove chromium from contaminated water. For nano-filtration a lower operating pressure is required than the reverse osmosis. Hosseini et al. (2017) fabricated nano-filtration membrane for Ni(II) and Cr(VI) removal. The material used for membrane synthesis was poly (acrylonitrile), poly(ethylene glycol) and TiO<sub>2</sub> as additive. Under optimized conditions, % rejection for nickel and chromium were 87 and 83%, respectively at the nickel concentration of 0.19 mM and for chromium concentration of 0.17 mM. Gaikwad and Balomajumder (2017) reported around 88 and 82%, respectively for chromium and fluorine using commercial composite polyamide membranes at initial Cr and F concentration 0.10 and 0.26 mM, respectively.

The membrane technologies also suffer from the generation of residual sludge lead to secondary pollution, are energy expensive, and regeneration and cleaning of the membrane add operational cost (Ortega et al. 2017).

In another study phytoremediation techniques were also employed to treat certain contaminant to reduce its toxicity. Sandana Mala et al. (2015) concluded that 91.3% Cr reduction could be achieved in 48 h by isolating *Bacillus methylotrophicus* from tannery sludge and using it against Cr(VI) reduction. Table 2.4 summarizes the techniques used for Cr(VI) removal.

**Table 2.4: Removal techniques and materials used for remediation of Cr(VI) from wastewater**

Material	Removal Technique	Results	Reference
Magnetic Graphene Nanocomposites	Adsorption	Removal % >95 % for Cr(VI) below pH 6	Zhu et al., 2012
Ti <sup>3+</sup> self-doped TiO <sub>2</sub>	Photocatalytic reduction	The reduction % of Cr(VI) is > 95%	Hao et al., 2019
Positively charged membrane	Ultrafiltration	Cr(VI) rejection >90%	Yao et al., 2015
Bentonite/chitosan@cobalt oxide	Adsorption and advanced oxidation	Congo red concentration was completely removed after 240 min and Cr(VI) concentration was removed after 360min	Abukhadra et al., 2019
Graphene oxide and polyaniline	Adsorption	The removal efficiency is increases from 31.6 to 66.2%	Shaban et al., 2018



		when GO dose increases from 25 to 150 mg	
Palladium nanoparticles supported on amine-functionalized SiO <sub>2</sub>	Catalytic reduction	Catalytic activity >85% after the 5th catalytic reuse at room temperature	Celebi et al., 2016
Titanium dioxide	Photocatalytic reduction	% reduction from Cr(VI) to Cr(III) ~ 98%	Ku and Jung 2001
Silver nanoparticles modified mesoporous silicon	Photocatalytic reduction	photo-reduction efficiency (97.4%) after 180 min was achieved under visible-light	Faisal et al., 2019
Polyamide skin over a polysulphone support	Nanofiltration followed by reverse osmosis	Retention of chromium is found to be 91–98% for NF and 98.8–99.7% for RO	Das et al., 2006
Coagulant - FeCl <sub>3</sub>	Filtration and	Cr(VI) removal	Chowdhury et al.,

	coagulation	was 96% at 150 mg dosage coagulant	2013
Polyacrylonitrile	Ultrafiltration	Rejection of $\geq 90\%$ was achieved for pH $\geq 7$ for Cr concentration $< 25$ ppm	Muthumareeswara n et al., 2016

## 2.6 PHOTO-CATALYTIC MEMBRANES AND THEIR APPLICATION

During the last two decades, the possibility of use of photo-catalysts for removal of pollutants has received attention of researchers due to their high chemical stability, low production cost, and the ability to use in a small percentage in the presence of ultraviolet light or solar radiation. Nano-particles of various pure or mixed semiconductors have been in used as photo-catalysts for removal of Cr(VI). The efficiency of photo-catalyst is dependent on various parameters including the initial concentration of contaminant, photon flux, presence /absence of oxygen, catalyst amount, solution pH, and temperature

The available publications on the removal/reduction of Cr(VI) mostly include use of heterogeneous photo-catalysis in suspended form for water treatment. The problems faced during separation of the catalysts from the solution led to the introduction of functionalization of polymeric supports (inert) with photo-catalysts in

order to avoid filtration step and easy reuse of the catalyst without compromising its stability. Incorporation of nano-material (photocatalyst) into polymer matrix leads to the development of a photo-catalytic membrane. Liu et al. (2012) fabricated a membrane composed of Ag/TiO<sub>2</sub> on glass fibre substrate for disinfection application under solar radiation. Ideally, integrating membranes with self-cleaning property via photo-catalytic oxidation/reduction is considered as one of the most promising technologies in terms of energy-efficiency and environmental view point (Zhou et al., 2012). Xu et al. (2016) develop a PVDF/TiO<sub>2</sub> membrane via the phase inversion technique to enhance the dye removal rate though the use of photo-catalyst. Lv et al. (2017a) deposited polydopamine (PDA)/polyethyleneimine (PEI) layer on an ultra-filtration membrane by co-deposition method followed by mineralization of a  $\beta$ -FeOOH nanorods as shown in Figure 2.4 for high efficiency degradation of dye (approx. 97.3% )under visible light irradiation even after 5 cycles.

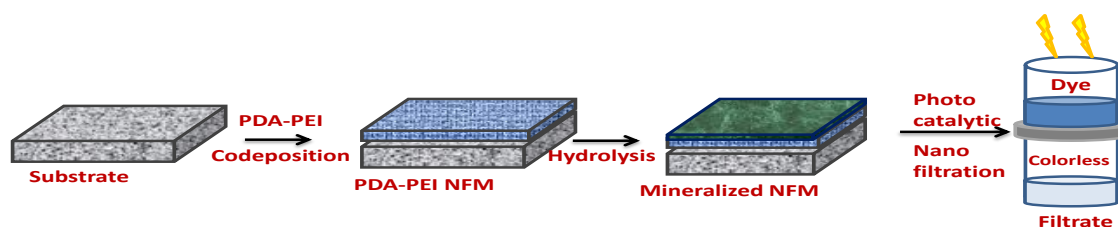


**Figure2.4: Schematic representation of nanofiltration photocatalytic membrane**

(Lv et al. 2017a)

Mozia et al. (2015) studied the effect of various parameters including nano-particle loading (0.5-1.5 g/dm<sup>3</sup>), feed flow (3-6 m/s), transmembrane pressure (1- 3 bar) on the performance, stability and fouling property of developed photo-catalytic membrane. Their-result revealed that selection of a proper feed cross flow velocity is important in enhancing the membrane flux. The abrasion of a membrane was most

probably the reason for the improvement in permeate flux which was attributed to the deposition of  $\text{TiO}_2$  photo-catalyst particles in the membrane pores. Coupling of separation and photo-catalytic degradation was considered as an interesting method (Djafer et al., 2010) because it simultaneously solves the membrane fouling problem and eliminates the molecules which are not readily removed using pristine membrane. The fabricated membrane was composed of active titania-based ultra-filtration membrane and alumina supports. The efficiency of membrane was measured by destroying the organic dye (methylene blue) in the range  $0.8\text{--}3.8 \times 10^{-8} \text{ mol s}^{-1} \text{ m}^{-2}$ .

A preliminary study was done by Molinari et al. (2017) for arsenic (As) removal by coupling photo-catalysis and ultra-filtration process. The schematic representation of the setup used is shown in Figure 2.5

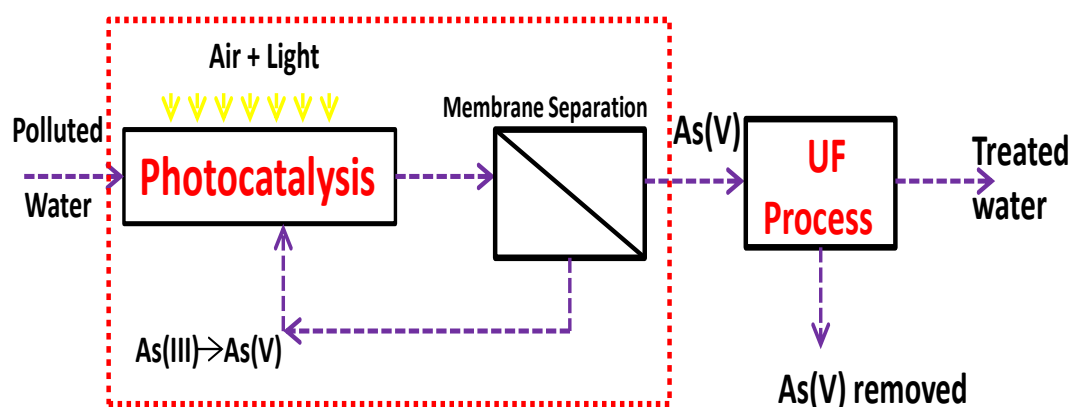


**Figure 2.5: Experimental setup representation for As removal**

(Molinari et al., 2017)

No As(III) removal was observed under operating conditions without pre-oxidation process. Thus ensuring that pre-oxidation is the necessary step, successful photo-catalytic oxidation of As(III) to As(V) was performed under UV radiation by using  $0.05 \text{ mg L}^{-1} \text{ TiO}_2$  photo-catalyst at pH 9 followed by microfiltration to separate As(V) containing water which was further removed from water by coupling an ultra-

filtration process. It was observed that at the end of 60 min at pH 4.5 a high conversion of 98.45% was achieved.

A photo-catalytic membrane was also tested against reduction chromium (VI) reduction as well as oxidation of EDTA using combining effect of photo-catalysis and cation exchange membrane (Hsu et al., 2013). The reduction efficiency increased due to presence of cation exchange membrane as it prevents re-oxidation of Cr(III) to Cr(VI) during photo-electrolytic process. The cation exchange membrane was an ion selective membrane so Cr(III) ion formed got accumulated towards the cathode on application of electric field. At pH 3, current density 4 mA/cm<sup>2</sup> and TiO<sub>2</sub> dosage of 1 g/L under UV illumination complete conversion of Cr (VI) in presence of EDTA was observed. The EDTA played the role of hole scavenger in the system. Kazemi et al. (2018) modified commercial thin film composite membrane via layer by layer technology using chitosan and photocatalytic nZVI@TiO<sub>2</sub> nanoparticle. Modified membrane showed enhancement in flux from 26.2 to 39.7 l/m<sup>2</sup> h increased flux recovery value from 62% to 87%. The Cr(VI) removal was greater than 95% on the permeate side. A similar technique was employed by to modify ultrafiltration membrane by using chitosan/alginate bilayers and Fe<sup>0</sup>@WO<sub>3</sub> nanoparticle (Kazemi et al., 2018) and it was observed that %rejection% increased from 21 to 99.2% at feed concentration of 5 mg/L, 17 to 91.8% at 25 mg/L and 9 to 78.1% at 50 mg/L compared to the pristine membrane.

Ong et al. (2019) investigated synergistic effect (solar photocatalysis + adsorption process) using Fe-doped ZnO and Fe-doped ZnO/rGO synthesized using sol-gel method to degrade Congo red. Performance of ZnO was found to be improved by doping with Fe and even better results were obtained when doped with rGO. A

comparative study of suspended and immobilized photo-catalytic membrane reactor was also carried out by Dzinum et al. (2019). Catalyst composed of TiO<sub>2</sub>/clinoptilolite was prepared using solid state dispersion technique and was embedded on the outer layer of hollow fibre membrane via single step co-spinning process. It was concluded that 86% degradation of reactive Black 5 was obtained including additional step required to separate the catalyst in 60 min. However in case of immobilized system degradation efficiency was less than the suspended form but at the same time 95% rejection was achieved under solar irradiation. Study on the dynamic photo-catalytic membranes (Figure 2.5) was done by Liu et al. (2020) in order to solve the problem associated with suspended form. The experimental results suggested that removal efficiency was significantly enhanced against fluvastatin and total organic carbon compared to pristine PVDF. Schematic representation of the setup used to carry out the experiment is shown in Figure 2.6. The removal efficiency of fluvastatin and TOC at optimal loading of ZnIn<sub>2</sub>S<sub>4</sub> (2.6 mg/cm<sup>2</sup>) were 97.19% and 53.29%, respectively.

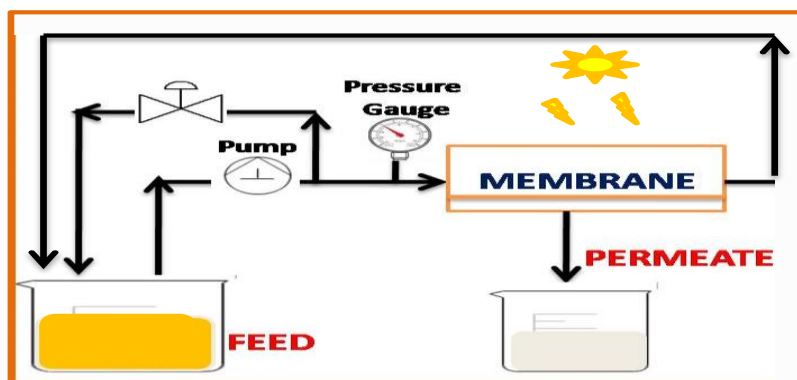


**Figure 2.6: Schematic representation of a photo-catalytic membrane reactor (Liu et al., 2020)**

A summary of available information on the the use of photo-catalytic membranes is listed in Table 2.5

Table 2.5: Use of photo-catalytic membranes for wastewater treatment

Material	Synthesized/ Commercial	Results	Reference
PSf/TiO <sub>2</sub>	Synthesized	<ul style="list-style-type: none"> <li>Reduction &gt;95% of Cr (VI) to Cr (III) perchloric acid within 2.0 h.</li> <li>Rejection &gt;65% at 200 KPa</li> </ul>	Jyothi et al., 2017
PSf/TiO <sub>2</sub>	Synthesized	<ul style="list-style-type: none"> <li>Reduction ~ 92% within 150 min</li> <li>rejection of up to 98%</li> </ul>	Jyothi et al., 2017
Tertiary amine groups were introduced into PVDF membrane	Synthesized	<ul style="list-style-type: none"> <li>Removal of almost 95% for Cr(VI)</li> </ul>	Yao et al., 2015
Nitrogen doped TiO <sub>2</sub>	Commercial (photocatalysis combining ionic exchange membrane)	<ul style="list-style-type: none"> <li>Removal of almost 95% for Cr(VI)</li> </ul>	Hsu et al., 2011
g-C <sub>3</sub> N <sub>4</sub> /TNA membrane	Synthesized	<ul style="list-style-type: none"> <li>Using integrated approach flux 2 times higher than using membrane alone</li> <li>Enhanced antifouling ability against <i>E.coli</i>.</li> </ul>	Zhang et al., 2017

		<ul style="list-style-type: none"> <li>Using synergistic approach</li> </ul> <p>&gt;60% Rhodamine B could be removed.</p>	
BiOBr (photocatalyst)/ polytetrafluoroethylene (membrane)	Synthesized photocatalyst	<ul style="list-style-type: none"> <li>Synergistic removal of 4-CP and Ag<sup>+</sup> ions.</li> <li>4-CP photo-oxidation was improved by Ag surface plasma effect.</li> </ul>	Zou et al., 2020
Amine-impregnated TiO <sub>2</sub> modified cellulose acetate membranes	Synthesized	<ul style="list-style-type: none"> <li>Model Cr solution: 72.4% rejection</li> </ul>	Alebel Gebru and Das, 2018
Anaerobic nano zero-valent iron granules	Synthesized	<ul style="list-style-type: none"> <li>Model Cr solution: 88 ± 1.56% rejection</li> </ul>	Venkatagi ri et. al., 2019

## 2.7 EFFECT OF NANO-PARTICLE LOADING ON THE PERFORMANCE OF MEMBRANES AND THEIR PHOTO-CATALYST APPLICATION

Nano-materials are usually embedded during membrane synthesis to develop mixed-matrix membrane with improved properties and performance. The stability and uniform dispersion of the nano-materials within the polymer matrix and need to use high ratio of nano-materials plays a major role for significant improvement of membrane properties and is considered as the major hurdle for commercialization. Mokhtari et al. (2017) incorporated salicylate-alumoxane nanoparticles in polysulfone



polymer matrix and observed that at 1% of salicylate-alumoxane, highest flux recovery of 87% was obtained. It was also concluded that further increase in loading to 2% the contact angle increased due to particle agglomeration at higher loading inducing more roughness to the membrane surface. A thin film composite membrane for forward osmosis application composed of halloysite/graphitic carbon nitride (g-C<sub>3</sub>N<sub>4</sub>) nanoparticles embedded in polysulfone substrate was fabricated by DashtArzhandi et al. (2018). The results obtained suggested that at 0.05 wt/v% of g-C<sub>3</sub>N<sub>4</sub> the contact angle reduced significantly from 68 to 10° and the flux enhanced approximately by 270% higher than the pristine polymer membrane (0 wt/v%). The findings ensure that addition of g-C<sub>3</sub>N<sub>4</sub> as a surface modifier contributes to the flux enhancement as well as enhancement in the anti-fouling properties. The effect of multi-walled carbon nano-tube on polyaniline was investigated by Bagheripour et al. (2016). The contact angle value decreased from 63 to 46 ° with increase in the loading from 0 to 0.1 wt% along with an increase in the salt rejection value and flux but further increase in the content to 1% showed a negative response.

Aluminium oxide entrapped PES membrane for ultra-filtration was developed using phase inversion technique by Maximous et al. (2009) to study the impact of polymer concentration on the performance and characteristic of membrane. It was concluded that 18% polymer concentration was considered as the optimum loading with respect to particle concentration. The permeability value was found to be increased 8 to 12 folds at this particular loading. Hairom et al. (2014) studied the effect of different loadings of ZnO on the performance of photo-catalyst membrane. It was observed that at optimum loading (0.3 g L<sup>-1</sup>) the maximum rejection and reduction of Congo red dye was observed at neutral pH. Maximous et al. (2010) varied loading of ZnO from 0 to 0.1

weight ratio with respect to polymer weight (PES) in study of to understand the effect of particle loading on the performance of a membrane bio- reactor. Increase in permeability of around 1.8 times higher than pure PES was observed. At the maximum loading a decrease in flux value was observed due to the clogging of pores.

In case of photo-catalyst application, the amount of photo-catalyst (nanoparticles) is of vital importance. Marikkani et al. (2019) reported that photo-reduction efficiency of increased with increase in  $\text{Fe}_2\text{V}_4\text{O}_{13}$  due to generation of large number of active sites thereby facilitating the adsorption process but above 50 mg loading, the particles aggregation results in the reduction of photo-reduction efficiency. The surface of PES was modified by doping oxygen-doped graphitic carbon nitride via phase inversion technique at room temperature. The amount of photo-catalyst was varied from 1 to 5 wt%. The results suggested that increase in loading from 0 to 4 wt% successfully increased the hydrophilicity with increase in the phenol rejection from 0.52 to 14.73% and reduction from 0 to 35.8%. However beyond 4% increase an opposite trend was observed and was attributed to the particle agglomeration, reduction in the active sites available to reject and reduce the pollutant concentration (Salim et al., 2019). Photo- degradation of Acid Yellow 36 was studied using photocatalysis–membrane distillation system (Mozia et al., 2009). Commercially available anatase phase  $\text{TiO}_2$  nano-particles were employed to degrade dye. The particle loadings varied from 0.1 to 0.5  $\text{g/dm}^3$  at 30  $\text{mg/dm}^3$  of initial concentration of the dye. It was mentioned that photo-catalyst concentration had a significant effect on the reduction%. The difference in the photo-degradation rate at 0.1 and 0.3  $\text{g TiO}_2/\text{dm}^3$  was greater than that at 0.3 and 0.5  $\text{g TiO}_2/\text{dm}^3$ . This is due to the fact that increase in catalyst loading increases the surface area (active site) for adsorption and degradation, but beyond optimum loading the particle-particle interaction becomes a dominant factor leading to

the agglomeration of particles thereby reducing the degradation rate. A hybrid multifunctional membrane consisting of PSf/TiO<sub>2</sub> was developed by Kuvarega et al. (2018) to evaluate the degradation of Eosin Yellow dye under sunlight. Particle concentration ranged between 0 to & 7 wt%. Increase in dye reduction from 67.3 to 97.3 % was obtained after 4 h irradiation. This was attributed to the increase in membrane porosity due to incorporation of nano-particle thus allowing faster solution permeation of the aqueous into the membrane.

Adán et al. (2017) designed a photo-catalysis/micro-filtration hybrid system to promote removal of bacteria for water disinfection applications. A synergistic effect including removal and photo-catalytic inactivation proved to be an efficient hybrid treatment technology. The reports suggested that pore size of membrane and particle loading played a major role in affecting the efficiency of the process. The experiments were carried out at different TiO<sub>2</sub> aqueous suspensions to achieve catalyst loadings in the range of 0–0.8 g per membrane. The reaction rates (methanol oxidation) improved with the increase of titanium dioxide and at 0.2–0.3 g of TiO<sub>2</sub> photo-catalytic activity reaches a plateau. Further increase in loading increases the internal mass transfer resistance again due to particle agglomeration thereby shielding the light reaching the surface and reducing the degradation efficiency.

## **2.8 CHALLENGES AND SHORTCOMINGS IN THE EXISTING WASTEWATER TREATMENT TECHNOLOGY**

Recent years, extensive efforts have been made to eliminate heavy metals discharged from industries and other sources from water streams. Various methods have been employed each having their advantages and limitations. Membrane technology proves to be potential technique for metallic ion removal. Different membrane

technologies include the Ultrafiltration membrane, various dense membrane including (nanofiltration, reverse osmosis, and Forward Osmosis), Liquid Membrane, and Electro Dialysis. Excluding Ultrafiltration other membrane technologies faces problem related high energy consumption due to high pressure driven process, expensive operational cost, concentration polarization. In case of low pressure driven process (ultrafiltration/microfiltration) suffers from low efficiency removal and also feed wastage is there in form of retentate hence additional step is required to treat the concentrated pollutant collected either on permeate or retentate side. Also the problem of easy fouling tendency restricts its successful application.

On other hand use of other emergent technology, advanced oxidation process (photocatalytic removal) although nowadays is used widely because of high efficiency removal due to large number of active site to degrade pollutant but poor recover ability increased additional cost to the system to separate photocatalyst material from the treated water. Coupling of membrane technology and photocatalyst (nanomaterial) could be an excellent method to eliminate pollutant without compromising cost and efficiency. Application of nanomaterial to induce synergistic effect to enhance the separation efficiency and reduction efficiency of polymeric composite has been explored and shown immense prospects. Still research is needed in this area to develop environment friendly materials for the synthesis of bifunctional membrane with excellent properties.

## **2.9 OBJECTIVE OF THE PRESENT WORK**

On the basis of the literature review it has become apparent that there is a need to explore the feasibility of photo-catalytic membrane based wastewater treatment technology for industries discharging toxic metallic and non-metallic ion bearing

effluents (e.g. those containing Cr(VI), Aresenate, etc.). In view of this present work has been planned with following objectives in mind:

- Synthesis of TiO<sub>2</sub> nanoparticles using green route based on extract of *Cajanus Cajan*
- Study of the phase behaviour and kinetic behaviour of casting solution use for making membranes
- Synthesis of polymer/TiO<sub>2</sub> composite membranes using different loading of TiO<sub>2</sub> nanoparticle
- Characterization of particles and membranes using X-Ray diffraction (XRD), Transmission Electron Microscope (TEM), Dynamic Light Scattering (DLS), Fourier Transform Infra Red Spectroscopy (FTIR), Contact Angle.
- Analysis of morphology, porosity, wettability, antibacterial and antifouling properties of membranes
- Application and comparative study of synthesized PVDF/TiO<sub>2</sub> membranes for removal of hexavalent chromium (Cr (VI)) from synthetic and real waste waters
- Optimization of process parameters (particle loading, pH, and Cr(VI) concentration ) for efficient membrane performance in terms of % Rejection and %Reduction.
- Application of response surface methodology(RSM) to optimize the parameter and validation with the experimental result at optimized condition.

## **2.9 REFERENCE**

Abukhadra MA, Adlii A, Bakry B Green fabrication of bentonite/chitosan@cobalt oxide composite (BE/CH@Co) of enhanced adsorption and advanced oxidation removal of Congo red dye and Cr (VI) from water. *International Journal of Biological Molecule* 126(2019)402-413

Acharya J, Sahu JN, Sahoo BK, Mohanty CR, Meikap BC Removal of chromium (VI) from wastewater by activated carbon developed from Tamarind wood activated with zinc chloride. *Chemical Engineering Journal* 150(2009) 25–39.

Adán C, Marugán J, Mesones S, Casado C, Grieken R Bacterial inactivation and degradation of organic molecules by titanium dioxide supported on porous stainless steel photocatalytic membranes. *Chemical Engineering Journal* 318(2017) 29-38.

Adeleke JT, Theivasanthi T, Thirupathi M, Swaminathan M, Akomolafe T Photocatalytic degradation of methylene blue by ZnO/NiFe<sub>2</sub>O<sub>4</sub> nanoparticles. *Applied Surface Science* 455, (2018) 195-200.

Agarwal H, Kumar SV, Rajeshkumar S A review on green synthesis of zinc oxide nanoparticles – An eco-friendly approach. *Resource-Efficient Technologies* 3 (2017) 406-413.

Ahmed S, Saifullah, Ahmad M, Swami B, Ikram S Green synthesis of silver nanoparticles using *Azadirachta indica* aqueous leaf extract. *Journal of Radiation Research and Applied Sciences* 9(2016) 1-7.

Ahmed MA, Ali SM El-Dek SI, Gala A Magnetite–hematite nanoparticles prepared by green methods for heavy metal ions removal from water. *Materials Science and Engineering: B* 178(2013)744-751.

AlebelGuru K Das C, Removal of chromium (VI) ions from aqueous solutions using amine-impregnated TiO<sub>2</sub>nanoparticles modified cellulose acetate membranes. Chemosphere 191 (2018) 673-684.

Alyarnezhad S, Marino T, Parsa JB, Galiano F, Ursino C, Garcia H, Puche M, Figoli A Polyvinylidene Fluoride-Graphene Oxide Membranes for Dye Removal under Visible Light Irradiation. Polymers 12(2020) 1509

Ambika S and Sundrarajan M Antibacterial behaviour of Vitex negundo extract assisted ZnO nanoparticles against pathogenic bacteria. Journal of Photochemistry and Photobiology B Biology 146 (2015)52-57

Amer W and Awwad A M Green Synthesis of copper nanoparticles by *Citrus limon* fruits extract, characterization and antibacterial activity. Chemistry International 7(1) (2021) 1-8

Anbuvarannan M, Ramesh M, Viruthagiri G, Shanmugam N, Kannadasan N *Anisochilus carnosus* leaf extract mediated synthesis of zinc oxide nanoparticles for antibacterial and photocatalytic activities. Material Science in Semiconductor Processing 39 (2015) 621-628.

Aromal SA and Philip D Green synthesis of gold nanoparticles using *Trigonellafoenum-graecum* and its size dependent catalytic activity Spectrochimica Acta A 97 (2012)1-5.

Atarod M, Nasrollahzadeh M, Sajadi SM, *Euphorbia heterophylla* leaf extract mediated green synthesis of Ag/TiO<sub>2</sub> nanocomposite and investigation of its excellent catalytic activity for reduction of variety of dyes in water. Journal of Colloid and Interface Science 462(2016) 272-279.

Atchudan R, Jebakumar TN, Edison I, Perumal S, Vinodh R, RokLee Y In-situ green synthesis of nitrogen-doped carbon dots for bio-imaging and

TiO<sub>2</sub> nanoparticles@nitrogen-doped carbon composite for photocatalytic degradation of organic pollutants. *Journal of Alloys and Compounds* 766(2018) 12-24.

Bagheripour E, Moghadassi A, Hosseini SM Preparation of mixed matrix PES-based nanofiltration membrane filled with PANI-co-MWCNT composite nanoparticles. *Korean Journal of Chemical Engineering* 33(4) (2016)1462-1471.

Berger LM, Stolle S, Gruner W, Wetzig K Investigation of the carbothermal reduction process of chromium oxide by micro- and lab-scale methods. *International Journal of Refractory Metals and Hard Materials* 19 (2001) 109–121.

Celebi M, Yurderi M, Bulut A, Kaya M, Zahmakiran M Palladium nanoparticles supported on amine-functionalized SiO<sub>2</sub> for the catalytic hexavalent chromium reduction. *Applied Catalysis B: Environmental* 180 (2016) 53–64.

Choudhary BC, Paul D, Gupta T, Tetgure SR, Garole VJ, Borse AU, Garole DJ Photocatalytic reduction of organic pollutant under visible light by green route synthesized gold nanoparticles. *Journal of Environmental Sciences* 55(2017) 236-246

Chowdhury M, Mostafa MG, Biswas TK, Saha AK Treatment of leather industrial effluents by filtration and coagulation processes *Water Resources and Industry* 3 (2013) 11–22.

Coto M, Troughton SC, Duan J, Kumar RV, Clyne TW Development and assessment of photo-catalytic membranes for water purification using solar radiation. *Applied Surface Science* 433 (2018) 101–107.

Damodar RA, You SJ, Chou HH Study the self-cleaning, antibacterial and photocatalytic properties of TiO<sub>2</sub> entrapped PVDF membranes *Journal of Hazardous Material* 172 (2009)1321-1328.



Daraei P, Madaeni SS, Salehi E, Ghaemi N, Ghari HS, Khadivi MA, Rostami E Novel thin film composite membrane fabricated by mixed matrix nanoclay/chitosan on PVDF microfiltration support: Preparation, characterization and performance in dye removal. *Journal of Membrane Science* 436(1) (2013) 97-108

Daraei P, Madaeni SS, Salehi E, Ghaemi N, Ghari HS, Khadivi MA, Rostami E, Astinchap B Novel polyethersulfone nanocomposite membrane prepared by PANI/Fe<sub>3</sub>O<sub>4</sub> nanoparticles with enhanced performance for Cu(II) removal from water. *Journal of Membrane Science* 415-416 (2012) 250-259

Das C, Patel P, De S, Gupta SD Treatment of tanning effluent using nanofiltration followed by reverse osmosis *Separation and Purification Technology* 50 (2006) 291–299.

Das J and Velusamy P Catalytic reduction of methylene blue using biogenic gold nanoparticles from *Sesbania grandiflora* L. *Journal of Taiwan Institute of Chemical Engineer* (2014)  
<https://doi.org/10.1016/j.jtice.2014.04.005>

DashtArzhandi MR, Sarrafzadeh MH, Goh PS, Lau WJ, Ismail AF, Mohamed MA Development of novel thin film nanocomposite forward osmosis membranes containing halloysite/graphitic carbon nitride nanoparticles towards enhanced desalination performance. *Desalination* 447(2018) 18-28.

Djafer L, Ayrala A, Ouagued A Robust synthesis and performance of a titania-based ultrafiltration membrane with photocatalytic properties. *Separation and Purification Technology* 75 (2010) 198–203

Dzinun H, Othman DH, Ismai AF, Photocatalytic performance of TiO<sub>2</sub>/Clinoptilolite: Comparison study in suspension and hybrid photocatalytic membrane reactor. *Chemosphere* 228(2019) 241-248

Devi B and Ahmaruzzaman M Bio-inspired facile and green fabrication of Au@Ag@AgCl core–double shells nanoparticles and their potential applications for elimination of toxic emerging pollutants: A green and efficient approach for wastewater treatment. *Chemical Engineering Journal* 317(2017) 726-741

Ebrahimian J, Mohsennia M, Khayatkashani M Photocatalytic-degradation of organic dye and removal of heavy metal ions using synthesized SnO<sub>2</sub> nanoparticles by *Vitex agnus-castus* fruit via a green route. *Materials Letters* 263(2020)127255

Ejraei A, Aroon A, Saravani AZ, Wastewater treatment using a hybrid system combining adsorption, photocatalytic degradation and membrane filtration processes *Journal of Water Process Engineering* 28 (2019) 45–53

Elumalai K, Velmurugan S, Ravi S, Kathiravan V, Ashokkumar S Green synthesis of zinc oxide nanoparticles using *Moringa oleifera* leaf extract and evaluation of its antimicrobial activity. *Spectrochimica Acta Part A Molecular and Biomolecular Spectroscopy* 143 (2015), 158-164

FazlzadehM, Rahmani K, Zarei A, Abdoallahzadeh H, Nasiri F, Khosravi R A novel green synthesis of zero valent iron nanoparticles (NZVI) using three plant extracts and their efficient application for removal of Cr(VI) from aqueous solutions. *Advanced Powder Technology* 28(1) (2017) 122-130

Faisal M, Harraz FA, Al Salami AE, ElToni AM, Almadhy AA, Khan A, Labis JP, Al-Sayari SA, Al-Assiri MS Enhanced photocatalytic reduction of Cr(VI) on silver nanoparticles modified mesoporous silicon under visible light. *Journal of American Chemical Society* (2019) 1-11

Fellenz N, Perez-Alonso FJ, Martin PP, García-Fierro JL, Bengoa JF, Marchetti SG, Rojas S Chromium (VI) removal from water by means of adsorption-reduction at the

surface of amino-functionalized MCM-41 sorbents. *Microporous and Mesoporous Materials* 239 (2017) 138-146.

Fowsiya J, Madhumitha G, Al-Dhabi NA, ValanArasu M Photocatalytic degradation of Congo red using *Carissa edulis* extract capped zinc oxide nanoparticles. *Journal of Photochemistry and Photobiology B: Biology* 162(2016) 395-401.

Fu L and Fu Z Plectranthusamboinicus leaf extract-assisted biosynthesis of ZnO nanoparticles and their photocatalytic activity. *Ceramic International* 41 (2015) 2492-2496

Gao Y, Hu M, Mi B Membrane surface modification with TiO<sub>2</sub>-graphene oxide for enhanced photocatalytic performance. *Journal of Membrane Science* 455(2014)349-356

Gaikwad MS, Balomajumder C Simultaneous rejection of chromium(VI) and fluoride [Cr(VI) and F] by nanofiltration: membranes characterizations and estimations of membrane transport parameters by CFSK model. *Journal of Environmental Chemical Engineering* 5(2017)45-53.

Geetha P Latha MS, Pillai SS, Deepa B, Kumar KS, Koshy M Green synthesis and characterization of alginate nanoparticles and its role as a biosorbent for Cr(VI) ions. *Journal of Molecular Structure* 1105(2016) 54-60

Ghaem N A new approach to copper ion removal from water by polymeric nanocomposite membrane embedded with  $\gamma$ -alumina nanoparticles. *Applied Surface Science* 364 (2016) 221-228

Ghaem N, Daraei P Enhancement in copper ion removal by PPy@Al<sub>2</sub>O<sub>3</sub> polymeric nanocomposite membrane. *Journal of Industrial and Engineering Chemistry* 40(2016) 26-33

Ghotekar S A review on plant extract mediated biogenic synthesis of CdO nanoparticles and their recent applications. *Asian journal of Green chemistry* 3(2019)187-200

Giannakas AE, Antonopoulou M, Deligiannakis Y, Konstantinou I Preparation, characterization of N-I co-doped TiO<sub>2</sub> and catalytic performance toward simultaneous Cr(VI) reduction and benzoic acid oxidation. *Applied Catalysis B Environment* 140(2013)636–645.

Gohari RJ, Lau WJ, Halakoo E, Ismail AF, Korminouri F, Matsuura T, Gohari MSJ, Chowdhury NK Arsenate removal from contaminated water by a highly adsorptive nanocomposite ultrafiltration membrane *New Journal of Chemistry* 39(2015)8263-8272.

Gong J-L, Wang B, Zeng Z-M, Yang C-P, Niu C-G, Niu QY, Zhou WJ, Liang Y Removal of cationic dyes from aqueous solution using magnetic multi-wall carbon nanotube nanocomposite as adsorbent. *Journal of Hazardous Materials* 164 (2009) 1517-1522.

Goutam SP, Saxena G, Singh V, Yadav AK, Bharagava RN, Thapa KB Green synthesis of TiO<sub>2</sub> nanoparticles using leaf extract of *Jatropha curcas* L. for photocatalytic degradation of tannery wastewater. *Chemical Engineering Journal* 336 (2018) 386-396.

Hairom NHH, Mohammad AW, Kadhum AAK Effect of various zinc oxide nanoparticles in membrane photocatalytic reactor for Congo red dye treatment. *Separation and Purification Technology* 137(2014) 74-81.

Hao W, Li X, Qin L, Han S, Kang S-Z Facile preparation of Ti<sup>3+</sup> self-doped TiO<sub>2</sub> nanoparticles and their dramatic visible photocatalytic activity for the fast treatment of highly concentrated Cr(VI) effluent. *Catalysis Science & Technology* 9(2019) 2523.

Hariharan D, Christy AJ, Mayandi J, Nehru LC Visible light active photocatalyst: Hydrothermal green synthesized TiO<sub>2</sub> NPs for degradation of picric acid *Materials Letters* 222, (2018) 45-49.

Ha TT , Quan VA , Hop NQ, Thuy TM , Ngoc NT , Que LX Studying on the adsorption of chromium (VI) on polyaniline modified with activated tea residue, *Vietnam J. Chem.* 56 (5) (2018) 559–563.

Hebbar RS, Isloor AM, Ismail AF Preparation and evaluation of heavy metal rejection properties of polyetherimide/porous activated bentonite clay nanocomposite membrane *RSC Advance* 4 (2014) 47240-47248.

Hosseini SS, Nazif A, Alaei Shahmirzadi MA, Ortiz I Fabrication, tuning and optimization of poly (acrylonitrile) nanofiltration membranes for effective nickel and chromium removal from electroplating wastewater. *Separation and Purification Technology* 187(2017)46–59.

Hsu H-T, Chen S-S, Chen Y-S Removal of chromium (VI) and naphthalene sulfonate from textile wastewater by photocatalysis combining ionic exchange membrane processes. *Separation and Purification Technology* 80 (2011) 663–669

Hsu H-T, Chen S-S, Teng Y-F, His H-C Enhanced photocatalytic activity of chromium(VI) reduction and EDTA oxidization by photoelectrocatalysis combining cationic exchange membrane processes. *Journal of Hazardous Materials* 248–249(2013) 97-106

Ijadpanah-Saravy H, Safari M, Khodadadi-Darban A, Rezaei A Synthesis of Titanium dioxide nanoparticles for photocatalytic degradation of cyanide in wastewater. *Analytical Letters*, 47(2014) 1772–1782.

Jyothi MS, Nayak V, Padaki M, Balakrishna RG Sunlight active PSf/TiO<sub>2</sub> hybrid membrane for elimination of chromium Journal of Photochemistry and Photobiology A: Chemistry 339 (2017) 89–94

Jyothi MS, Nayak V, Padaki M, Balakrishna RG, Soontarapa K Eco-friendly membrane process and product development for complete elimination of chromium toxicity in wastewater. Journal of Hazardous Materials 332 (2017) 112–123

Jung G, Kim H Synthesis and Photocatalytic Performance of PVA/TiO<sub>2</sub>/Graphene-MWCNT Nanocomposites for Dye Removal. Journal of Applied Polymer Science (2014)40715-40722.

Kalaiselvi A, Roopan SM, Madhumitha G et al Synthesis and characterization of palladium nanoparticles using *Catharanthus roseus* leaf extract and its application in the photo-catalytic degradation. Spectrochimica Acta Part A Molecular and Biomolecular Spectroscopy (2015). <https://doi.org/10.1016/j.saa.2014.07.010>

Kanan S, Moyet MA, Arthur RB, Patterson HH, Recent advances on TiO<sub>2</sub> based photocatalysts toward the degradation of pesticides and major organic pollutants from water bodies. Catalysis Reviews (2019) <https://doi.org/10.1080/01614940.2019.1613323>

Karim Z, Mathew A, Grahn M, Mouzon J, Oksman K Nanoporous membranes with cellulose nanocrystals as functional entity in chitosan: Removal of dyes from water. Carbohydrate Polymers 112(4) (2014) 668-676.

Karim Z, Mathew AP, Kokol V, Wei J, Grahn M High-flux affinity membranes based on cellulose nanocomposites for removal of heavy metal ions from industrial effluents. RSC Advance 6 (2016)20644-20653

Kazi MA, Memon ZA, Shah FA, Ali ZM Exploration of Dye Degradation Potential of Eco-friendly Synthesized TiO<sub>2</sub> Nanoparticles Using Extract of *Acacia nilotica*. Pakistan Journal of Analytical & Environment Chemistry 20(2019) 135-140.

Kazemi M, Jahanshahi M, Peyravi M Chitosan-sodium alginate multilayer membrane developed by Fe<sup>0</sup>@WO<sub>3</sub> nanoparticles: Photocatalytic removal of hexavalent chromium. Carbohydrate Polymers 198(2018) 164-174.

Khan ZU, Khan A, Shah A, Wan P, Chen Y, Khan GM, Khan AU, Tahir K, Muhammad N, Khan HU Enhanced photocatalytic and electrocatalytic applications of green synthesized silver nanoparticles. Journal of Molecular Liquids 220(2016) 248-257.

Khosravi R, Ehrampoush MH, Moussavi G, Ghaneian MT, Barikbin B, Ebrahimi AA, Sharifzadeh G Facile green synthesis of zinc oxide nanoparticles using *Thymus vulgaris* extract, characterization, and mechanism of chromium photocatalytic reduction Materials Research Express, 6(2019) 115093.

Kononova ON, Bryuzgina GL, Apchitaeva OV, Kononov YS Ion exchange recovery of chromium (VI) and manganese (II) from aqueous solutions. Arabian Journal of Chemistry 12 (2015) 2713-2720.

Ku Y and Jung IL Photocatalytic Reduction of Cr (VI) in aqueous solutions by UV irradiation with the presence of Titanium Dioxide. Water Research 35 (2001) 135-142.

Kumar A and Jena HM Adsorption of Cr(VI) from aqueous phase by high surface area activated carbon prepared by chemical activation with ZnCl<sub>2</sub>. Process Safety and Environmental Protection 109(2017) 63–71.

Kumar PA, Ray M, Chakraborty S Hexavalent chromium removal from wastewater using aniline formaldehyde condensate coated silica gel. Journal of Hazardous Material 143(2007)24–32.

Kumar R, Singh RD, Sharma KD Water resources of India. *Current Science* 85(5) (2005) 794-811.

Kuvarega AT, Khumalo N, Dlamini D, Mamba BB Polysulfone/N,Pd co-doped TiO<sub>2</sub> composite membranes for photocatalytic dye degradation. *Separation and Purification Technology* 191(2018) 122-133.

Liu L, Liu Z, Bai H, Sun DD Concurrent filtration and solar photocatalytic disinfection/degradation using high-performance Ag/TiO<sub>2</sub> nanofiber membrane. *Water Research* 46 (2012)1101-1112.

Liu T, Wang L, Liu X, Sun C, Lv Y, Miao R, Wang X Dynamic photocatalytic membrane coated with ZnIn<sub>2</sub>S<sub>4</sub> for enhanced photocatalytic performance and antifouling property. *Chemical Engineering Journal* 379(2020) 122379.

Liu X, Jiang B, Ma H, Hsiao BS Highly permeable nanofibrous composite microfiltration membranes for removal of nanoparticles and heavy metal ions. *Separation and Purification Technology* 233 (2020) 115976

Lv Y, Zhang C, He A, Yang S-J, Wu G-P, Darling SB, Xu Z-K Photocatalytic Nanofiltration Membranes with Self-Cleaning Property for Wastewater Treatment. *Advanced Functional Material* 27(2017) 1700251.

Magudieshwaran R, Ishii J, Raja KCN, Terashima C, Venkatachalam R, Fujishima A, Pitchaimuthu S Green and chemical synthesized CeO<sub>2</sub> nanoparticles for photocatalytic indoor air pollutant degradation. *Materials Letters* 239, (2019) 40-44.

Mahmoudian M , Balkanloo PG, Nozad E A Facile Method for Dye and Heavy Metal Elimination by pH Sensitive Acid Activated Montmorillonite/Polyethersulfone Nanocomposite Membrane. *Chinese Journal of Polymer Science* 2018, 36, 49–57



Manikandan V, Jayanthi P, Priyadharsan A, Vijayaprathap E, Anbarasan PM, Velmurugan P Green synthesis of pH-responsive Al<sub>2</sub>O<sub>3</sub> nanoparticles: Application to rapid removal of nitrate ions with enhanced antibacterial activity. *Journal of Photochemistry and Photobiology A: Chemistry* 371(2019) 205-215

Marikkani S, Vinoth Kumar J, Muthuraj V Design of novel solar-light driven sponge-like Fe<sub>2</sub>V<sub>4</sub>O<sub>13</sub> photocatalyst: A unique platform for the photoreduction of carcinogenic hexavalent chromium. *Solar Energy* 188 (2019) 849–856

Marinho BA, Djellabi R, Cristóvão RO, Loureiro JM, Boaventura RAR, Dias MM, Carlos J, Lopes B, Vilar VJP Intensification of heterogeneous TiO<sub>2</sub> photocatalysis using an innovative micro–meso-structured-reactor for Cr(VI) reduction under simulated solar light. *Chemical Engineering Journal* 318(2017b) 76–88.

Martins PM, Miranda R, Marques J, Tavares CJ, BotelhoG, Lanceros-Mendez S Comparative efficiency of TiO<sub>2</sub> nanoparticles in suspension vs. immobilization into P(VDF–TrFE) porous membranes. *Royal Society of Chemistry Adv.*, 6 (2016)12708-12716.

Maximous N, Nakhla G, Wan W, Wong K Preparation, characterization and performance of Al<sub>2</sub>O<sub>3</sub>/PES membrane for wastewater filtration. *Journal of Membrane Science* 341(1–2) (2009) 67-75.

Maximous N, Nakhla G, Wan W, Wong K Performance of a novel ZrO<sub>2</sub>/PES membrane for wastewater filtration. *Journal of Membrane Science* 352(1–2) (2010) 222-230.

Meichtry JM, Colbeau-Justin C, Custo G, Litter MI Preservation of the photocatalytic activity of TiO<sub>2</sub> by EDTA in the reductive transformation of Cr(VI). *Studies by Time Resolved Microwave Conductivity Catalysis. Today* 224(2014a) 236–243.

Meichtry JM, Colbeau-Justin C, Custo G, Litter MI TiO<sub>2</sub>-photocatalytic transformation of Cr(VI) in the presence of EDTA: comparison of different commercial photocatalysts and studies by time resolved microwave conductivity. *Applied Catalysis B Environment* 144(2014b) 189–19.

Moradihamedani P, Kalantari K, Abdullah AH, Morad NA High efficient removal of lead(II) and nickel(II) from aqueous solution by novel polysulfone/Fe<sub>3</sub>O<sub>4</sub>-talc nanocomposite mixed matrix membrane. *Desalination and water treatment* 57(2016)28900-28909.

Mokhtari S, Rahimpour A, Shamsabadi AA, Habibzadeh S, Soroush M Enhancing performance and surface antifouling properties of polysulfone ultrafiltration membranes with salicylate-alumoxane nanoparticles. *Applied Surface Science* 393( 2017) 93-102.

Muthukumar H, Shanmugam MK, Gummadi SN Caffeine degradation in synthetic coffee wastewater using silverferrite nanoparticles fabricated via green route using *Amaranthus blitum* leaf aqueous extract. *Journal of Water Processing* 36(2020)101382

Mull B, Möhlmann L, Wilke O Photocatalytic Degradation of Toluene, Butyl Acetate and Limonene under UV and Visible Light with Titanium Dioxide-Graphene Oxide as Photocatalyst. *Environments* 4(2017)1 - 9

Muthumareeswaran MR, Alhoshan M, Agarwal GP. Ultrafiltration membrane for effective removal of chromium ions from potable water. *Scientific Reports* 7(2017) 41423.

Naseer M, Aslam U, Khalid B, Chen B Green route to synthesize Zinc Oxide Nanoparticles using leaf extracts of *Cassia fistula* and *Melia azadarach* and their

antibacterial potential. *Scientific Reports* 9055(2020) <https://doi.org/10.1038/s41598-020-65949-3>.

Narasaiah BP, Mandal BK Remediation of azo-dyes based toxicity by agro-waste cotton boll peels mediated palladium nanoparticles. *Journal of Saudi Chemical Society* 24(2020)267–281.

Nawaz H, Umar M, Ullah A, Razzaq H, Zia KM, Liu X Polyvinylidene fluoride nanocomposite super hydrophilic membrane integrated with Polyaniline-Graphene oxide nano fillers for treatment of textile effluents. *Journal of hazardous Material* 403(2021)123587

Ong CB, Wahab A, Ng LY Integrated adsorption-solar photocatalytic membrane reactor for degradation of hazardous Congo red using Fe-doped ZnO and Fe-doped ZnO/rGO nanocomposites. *Environmental Science and Pollution* 26(2019)33856–33869.

Ortega A, Oliva I, Contreras KE, González I, Cruz-Díaz MR, Rivero EP Arsenic removal from water by hybrid electro-regenerated anion exchange resin/electrodialysis process. *Separation and Purification Technology* 184(2017)319–326.

Patidar V and Jain P Green Synthesis of TiO<sub>2</sub> Nanoparticle Using Moringa Oleifera Leaf Extract. *International Research Journal of Engineering and Technology* 4(3) (2017) 470-473.

Pawar V, Kumar M, Dubey PK, Singh MK, Sinha ASK, Singh P, Influence of synthesis route on structural, optical and electrical properties of TiO<sub>2</sub>. *Applied Physics A* 125 (2019)657.

Peyravi M, Jahanshahi M, Rahimpour A, Javadi A, Hajavi S Novel thin film nanocomposite membranes incorporated with functionalized TiO<sub>2</sub> nanoparticles for organic solvent nanofiltration. *Chemical Engineering Journal* 241(2014) 155-166.

Prasad AR, Ammal PR, Joseph A Effective photocatalytic removal of different dye stuffs using green synthesized zinc oxide nanogranules. *Materials Research Bulletin* 102(2018)116-121.

Prasad AR, Garvavis J, Oruvil SK, Joseph A Bio-inspired green synthesis of zinc oxide nanoparticles using *Abelmoschus esculentus* mucilage and selective degradation of cationic dye pollutants. *Journal of Physics and Chemistry of Solids* 127(2019)265-274.

Rahimpour A, Madaeni SS, Taheri AH, Mansourpanah Y Coupling TiO<sub>2</sub> nanoparticles with UV irradiation for modification of polyethersulfone ultrafiltration membranes *Journal of Membrane Science* 313 (2008) 158-169

Rai MK, Shahi G, Meena V, Meena R, Chakraborty S, Singh RS, Rai BN Removal of hexavalent chromium Cr(VI) using activated carbon prepared from mango kernel activated with H<sub>3</sub>PO<sub>4</sub>. *Resource Technology* 2(2016) S63–S70.

Rani M and Shanker U, Removal of chlorpyrifos, thiamethoxam, and tebuconazole from water using green synthesized metal hexacyanoferrate nanoparticles. *Environmental Science and Pollution Research* 25(2018) 10878–10893.

Reddy PVL and Kim K-H, A review of photochemical approaches for the treatment of a wide range of pesticides. *Journal of Hazardous Material* 285 (2015) 325-335.

Salim NE, Nor NAM, Jaafar J, Ismail AF, Qtaishat MR, MHD, Rahman MA, Aziz F, N.Yusof Effects of hydrophilic surface macromolecule modifier loading on PES/O-g-C<sub>3</sub>N<sub>4</sub> hybrid photocatalytic membrane for phenol removal. *Applied Surface Science* 465(2019) 180-191.

Sandana Mala JG, Sujatha D, Rose C Inducible chromate reductase exhibiting extracellular activity in *Bacillus methylotrophicus* for chromium bioremediation. *Microbiological Research* 170(2015) 235–241

Sethy NK, Arif Z, Mishra PK, Kumar P (2020) Green synthesis of TiO<sub>2</sub> nanoparticles from *Syzygium cumini* extract for photo-catalytic removal of lead (Pb) in explosive industrial wastewater. *Green Processing Synthesis* 9 (2020) 171-181

Shaban M, Abukhadra MR, Rabia M, Elkader YA, Abd El-Halim MR Investigation the adsorption properties of graphene oxide and polyanilineno/micro structures for efficient removal of toxic Cr(VI) contaminants from aqueous solutions; kinetic and equilibrium studies *Rendiconti Lincei. ScienzeFisiche e Naturali* 29 (2018)141–154.

Shabani M, Rahaiee, Zare M, Jafari SM Green synthesis of ZnO nanoparticles using loquat seed extract; Biological functions and photocatalytic degradation properties. *LWT* 134 (2020)110133

Shah P, Murthy CN Studies on the porosity control of MWCNT/polysulfone composite membrane and its effect on metal removal. *Journal of Membrane Science* 437(2013) 90-98.

Sharma D, Kanchi S, Bisetty K Biogenic synthesis of nanoparticles: A review. *Arabian Journal of Chemistry* 12(2019) 3576-3600.

Shanker U, Jassal V, Rani M Green synthesis of iron hexacyanoferrate nanoparticles: Potential candidate for the degradation of toxic PAHs. *Journal of Environmental Chemical Engineering* 5(2017) 4108-4120.

Sheik Mydeen S, Raj Kumar R, Kottaisamy M, Vasantha VS Biosynthesis of ZnO nanoparticles through extract from *Prosopisjuliflora* plant leaf: antibacterial activities and a new approach by rust-induced photocatalysis. *Journal of Saudi Chemical Society* 24 (2020) 393–406

Singh J, Kumar V, Kim K-H, Rawat M Biogenic synthesis of copper oxide nanoparticles using plant extract and its prodigious potential for photocatalytic degradation of dyes. *Environmental Research* 177(2019)108569

Souza F, Brandão HL, Hackbarth FG, Souza AAU, Boaventura RAR, Souza SMAGU, Vilar VJP Marine macro-alga *Sargassum cymosum* as electron donor for hexavalent chromium reduction to trivalent state in aqueous solutions. *Chemical Engineering Journal* 283(2016) 903-910.

Singh J, Kaur N, Kaur P, Kaur S, Kaur J, Kukkar P, Kumar V, Kukkar D, Rawat M *Piper betle* leaves mediated synthesis of biogenic SnO<sub>2</sub> nanoparticles for photocatalytic degradation of reactive yellow 186 dye under direct sunlight *Environmental Nanotechnology, Monitoring & Management* 10(2018) 331-338.

Srikar SK, Giri DD, Pal DB, Mishra PK, Upadhyay SN, Green synthesis of silver nanoparticles: A review. *Green and Sustainable Chemistry* 6(2016) 34-56.

Srinivasan M, Venkatesan M, Arumugam V, Natesan G, Saravanan N, Murugesan S, Ramachandran S, Ayyasamy R, Pugazhendhi A Green synthesis and characterization of titanium dioxide nanoparticles (TiO<sub>2</sub> NPs) using *Sesbania grandiflora* and evaluation of toxicity in zebrafish embryos. *Process Biochemistry* 80(2019) 197-202

Tamuly C, Hazarika M, Bordoloi M Biosynthesis of Au nanoparticles by *Gymnocladus assamicus* and its catalytic activity. *Material Letter* (2013) <https://doi.org/10.1016/j.matlet.2013.07.020>

Testa JJ, Grela MA, Litter MI Heterogeneous photocatalytic reduction of chromium(VI) over TiO<sub>2</sub> particles in the presence of oxalate: involvement of Cr(VI) species. *Environmental Science and Technology* 38(2004)1589–1594.

Tezcan Un U, Onpeker SE, Ozel E The treatment of chromium containing wastewater

using electrocoagulation and the production of ceramic pigments from the resulting sludge. *Journal of Environmental Management* 200(2017)196–203

Thandapani K, Kathiravan M, Namasivayam E, Padiksan IA, Natesan G, Tiwari M, Giovanni B Perumal V, Enhanced larvicidal, antibacterial, and photocatalytic efficacy of TiO<sub>2</sub>nanohybrids green synthesized using the aqueous leaf extract of *Parthenium hysterophorus*. *Environmental Science Pollution Research* 25(2018)10328–10339

Thong Z, Han G, Cui Y, Gao J, Chung T-S, Chan S-Y, Wei S Novel Nanofiltration Membranes Consisting of a Sulfonated Pentablock Copolymer Rejection Layer for Heavy Metal Removal. *Environmental Science and Technology* 48(2014)13880–13887

VenkataGiri RK, Raju LS, Nancharaiah YV, Pulimi M, Chandrasekaran N, Mukherjee A , Anaerobic nano zero-valent iron granules for hexavalent chromium removal from aqueous solution. *Environmental Technology and Innovation* 16 (2019) 100495-100507

Wang Z, Fang C, Megharaj M Characterization of iron–polyphenol nanoparticles synthesized by three plant extracts and their fenton oxidation of azo dye. *ACS Sustainable Chemistry and Engineering* 2 (4) (2014) 1022-1025

Wang T, Wang M, Wang P, Tang Y An integration of photo-Fenton and membrane process for water treatment by a PVDF@CuFe<sub>2</sub>O<sub>4</sub> catalytic membrane *Journal of Membrane Science* 572 (2019) 419–427.

Wang Y, Zhu J, Dong G, Zhang Y, Guo N, Liu J Sulfonated halloysite nanotubes/polyethersulfone nanocomposite membrane for efficient dye purification. *Separation and Purification Technology* 150(17) (2015) 243-251.

Wang Z, Que B, Gan J, Chen Q, Zheng L, Marraiki N, Elgorban AM, Zhang Y Zinc oxide nanoparticles synthesized from *Fraxinus rhynchophylla* extract by green route method attenuates the chemical and inflammatory pain models in mice. *Journal of Photochemistry and Photobiology B: Biology* 202(2020)111668

Weng X, Jin X, Lin J, Naidu R, Chen Z Removal of mixed contaminants Cr (VI) and Cu(II) by green synthesized iron based nanoparticles. *Ecological Engineering*97(2016) 32-39

Xu Z, Wu T, Shi J, Teng K, Wang W, Ma M, Li J, Qian X, Li C, Fan J Photocatalytic antifouling PVDF ultrafiltration membranes based on synergy of graphene oxide and TiO<sub>2</sub> for water treatment. *Journal of Membrane Science* 520 (2016) 281–293

Xu J, Li Y, Yuan B, Shen C, Fu M, Cui H, Sun W, Large scale preparation of Cu-doped  $\alpha$ -FeOOH nanoflowers and their photo-Fenton-like catalytic degradation of diclofenac sodium. *Chemical Engineering Journal* 291(2016)174-183.

Xue Y, Zheng S, Sun Z, Zhang Y, Jin W, Alkaline electrochemical advanced oxidation process for chromium oxidation at graphitized multi-walled carbon nanotubes. *Chemosphere* 183 (2017) 156-163

Yallappa S, Manjanna J, Dhananjaya BL, Phytosynthesis of stable Au, Ag and Au–Ag alloy nanoparticles using *J. sambac* leaves extract, and their enhanced antimicrobial activity in presence of organic antimicrobials. *Spectrochimica Acta part A: Molecular and Biomolecular Spectroscopy* 137 (2015) 236-243

Yao Z, Li Y, Cui Y, Zheng K, Zhu B, Xu H, Zhu L, Tertiary amine block copolymer containing ultrafiltration membrane with pH-dependent macromolecule sieving and Cr(VI) removal properties *Desalination* 355 (2015) 91–98

Yao Z, Du S, Zhang Y, Zhu B, Zhu L, John AE, Positively charged membrane for removing low concentration Cr(VI)in ultrafiltration process. *Journal of Water Process Engineering*8(2015)99–107.

Yang L, Wang Z, Zhang J, Zeolite imidazolate framework hybrid nanofiltration (NF)



membranes with enhanced permselectivity for dye removal. *Journal of Membrane Science* 532(2017) 76-86.

Zak S, Treatment of the processing wastewaters containing heavy metals with the method based on flotation, *Ecological Chemistry and Engineering S* 19 (2012) 433–438.

Zhou X, Lan J, Liu G, Deng K, Yang Y, Nie G, Yu J, Zhi L, facet-mediated photodegradation of organic dye over hematite architectures by visible light. *Angewandte. Chemie International Edition* 51(2012)178-182

Zhang C, Wei K, Zhang W, Bai Y, Sun Y, Guz J, Graphene Oxide Quantum Dots Incorporated into a Thin Film Nanocomposite Membrane with High Flux and Antifouling Properties for Low-Pressure Nanofiltration. *ACS Applied Material Interfaces*9(2017)11082–11094.

Zhang Q, Quan X, Wang H, Chen S, Su Y, Li Z, Constructing a visible-light-driven photocatalytic membrane by g-C<sub>3</sub>N<sub>4</sub> quantum dots and TiO<sub>2</sub> nanotube array for enhanced water treatment. *Scientific Reports* 7(2017) 3128.

Zhang X, Wang DK, Diniz da JC Costa, Recent progresses on fabrication of photocatalytic membranes for water treatment. *Catalysis Today* 230 (2014) 47–54.

Zhang Y, Zhang S, Chung T-S, Nanometric Graphene Oxide Framework Membranes with Enhanced Heavy Metal Removal via Nanofiltration. *Environmental Science and Technology* 49(2015)10235–10242.

Zhu J, Wei S, Gu H, Rapole SB, Wang Q, Luo Z, Haldolaarachchige N, Young DP, Guo Z One-Pot Synthesis of Magnetic Graphene Nanocomposites Decorated with Core@Double-shell Nanoparticles for Fast Chromium Removal. *Environmental Science and Technology* 46 (2012) 977–985.

Zinadini S, Zinatizadeh AA, Rahimi M, Vatanpour V, Zangeneh H, Beygzadeh M  
Novel high flux antifouling nanofiltration membranes for dye removal containing  
carboxymethyl chitosan coated Fe<sub>3</sub>O<sub>4</sub> nanoparticles. *Desalination* 349 (2014)145-154.

Zou Q, Zhang Z, Li H, Pei W, Ding M, Xie Z, Huo Y, Li H Synergistic removal of  
organic pollutant and metal ions in photocatalysis-membrane distillation system.  
*Applied Catalysis B: Environmental* 264(2020) 118463.